Appendix III

Amino acid racemization analysis

Kirsty Penkman & Matthew Collins

History of amino acid dating

The presence of proteins in archaeological remains has been known for some time; nearly fifty years ago Abelson (1954) separated amino acids from subfossil shell. He suggested the possibility of using the kinetics of the degradation of amino acids as the basis for a dating method (Abelson, 1955). In the mid-1960s Hare and Abelson measured the extent of degradation by racemization of amino acids extracted from modern and sub-fossil *Mercenaria mercenaria* (edible clam) shells. They found that the total amount of amino acids present decreased with the age of the shell and that, while the amino acids in recent shell were all in the L-configuration, over time the amount of D-configuration amino acid increased as a result of racemization (Hare & Abelson, 1967). This chemical reaction is the basis of Amino Acid Racemization (AAR) dating. However, even after 35 years this method is still subject to vigorous debate, with its application to date bone being particularly controversial (Bada, 1990; Marshall, 1990). Detailed reviews of AAR include those by Schroeder and Bada (1976), Bada (1991), Murray-Wallace (1993), Rutter and Blackwell (1995), Johnson and Miller (1997) and Hare *et al*. (1997).

The rate of racemization is influenced by a number of factors, including amino acid structure, the sequence of amino acids in peptides, pH, buffering effects, metallic cations, the presence of water and temperature. To establish a dating method the kinetics and mechanisms of the racemization reaction of free- and peptide-bound amino acids need to be established. To this end, various workers in the late 1960s and the 1970s studied free amino acids in solution and carried out laboratory simulations of post-mortem changes in the amino acids in bone (Bada, 1972) and shell (Hare & Abelson, 1967; Hare & Mitterer, 1969). Attempts have also been made to relate the kinetics of free amino acids to those in short polypeptides and the proteins in various archaeological samples (Bada, 1982; Smith & Evans, 1980). The suitability of this technique as a geochronological and geothermometry tool has led to its use in many environmental studies, on a range of substrates, from terrestrial gastropods (e.g. Goodfriend, 1991; 1992), bivalves (e.g. Goodfriend & Stanley, 1996), foraminifera (Harada *et al*., 1996), ostrich egg shells (Miller *et al*., 1992, 1997) and speleothems (Lauritzen *et al*., 1994). Early methods of chemical separation, using Ion-Exchange

Liquid Chromatography, were able to separate the enantiomers of one amino acid found in proteins, L-isoleucine (L-Ile, I), from its most stable diastereoisomer alloisoleucine (D-aile, A). By analysing the total protein content within mollusc shells from interglacial sites, an amino acid geochronology begun to be developed for the UK using the increase in A/I observed (Miller *et al*., 1979; Andrews *et al*., 1979), with correlations made with the marine oxygen isotope warm stages (Bowen *et al*., 1989).

New methodology

A new technique of amino acid analysis has been developed for geochronological purposes (Penkman, 2005; Penkman *et al*., 2008a), combining a new Reverse-Phase High Pressure Liquid Chromatography method of analysis (Kaufman & Manley, 1998) with the isolation of an 'intra-crystalline' fraction of amino acids by bleach treatment (Sykes *et al*., 1995). This combination of techniques results in the analysis of D/L values of multiple amino acids from the chemically-protected protein within the biomineral; enabling both decreased sample sizes and increased reliability of the analysis. Amino acid data obtained from the intra-crystalline fraction of the calcitic *Bithynia* opercula has been found to be a particularly robust repository for the original protein (Penkman *et al*., 2008b; in press). This has enabled an increased level of resolution and therefore this material has been focused on in this study.

This new technique has enabled amino acid dating to be used as an important comparative technique for materials dating back as far as the early Middle Pleistocene (e.g. Parfitt *et al*., 2005). Relatively few data have hitherto been obtained from calcite opercula from Holocene contexts, however, so the Swale Ure samples were viewed as an opportunity to extend the methodology while, at the same time, providing a further dating proxy for the Swale–Ure project. There was also the opportunity to date aragonite shells, as used in earlier applications of amino acid dating, although again this used the revised methodology developed by the authors.

Theory

Amino acids, the building blocks of proteins, occur as two isomers that are chemically identical, but optically different. These isomers are designated as either D (dextrorotary) or L (laevorotary), depending upon whether they rotate plane polarized light to the right or left respectively (Fig. 1). In living organisms the amino

acids in protein are almost exclusively L and thus the D/L value approaches zero[1]. The potential application to geochronology arises from the fact that, after death, amino acid isomers start to interconvert. This process is commonly termed racemization. In time the D/L value approaches one. The proportion of D to L amino acids is therefore an estimate of the extent of protein degradation and, if this is assumed to be predictable over time, it can be used to estimate age.

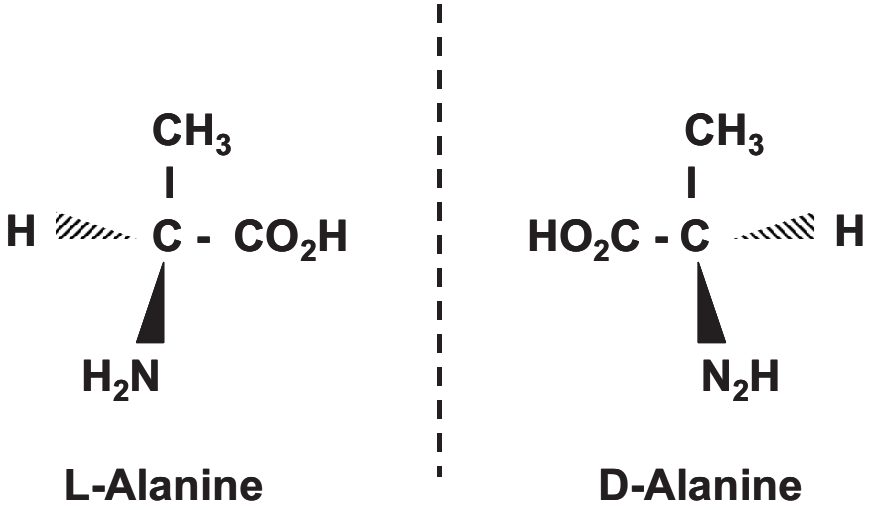

Figure 1: L- and D- amino acid structure

Mechanisms of racemization

The rate of racemization is governed by a variety of factors, most of which have been studied in detail only for free amino acids. The North East amino acid racemization (NEaar) laboratory analyses the intra-crystalline amino acid fraction and thus ensures that, within a closed environment in which other factors (water content, concentration of cations, pH) are constant, the extent of racemization is a function of time and temperature. Over a small geographical area such as that represented in the Swale–Ure project, it can be assumed that the integrated temperature histories are effectively the same. Any differences in the extent of decomposition of protein within the sample are therefore age-dependent.

Intra-crystalline protein decomposition

The organic matter existing within individual crystals (intra-crystalline fraction) is believed to be a more reliable substrate for analysis than the whole shell (Sykes *et al*., 1995; Penkman, 2005; Penkman *et al*., 2008a). The initial bleaching step in the recovery of the intra-crystalline fraction removes both secondary contamination and

[1] D-amino acids are synthesized by some organisms; they are found free in invertebrate body fluids where they play a role in osmoregulation and can occur peptide bound in bacterial peptidoglycan, where part of their function is resistance to proteases.

the organic matrix of the shell. This organic matrix degrades and leaches at an unpredictable rate over time, leading to variation in the concentration and D/L of the amino acids. Thus, as appears to be the case in ostrich eggshell (Miller *et al*., 2000), the D/L values of amino acids in the intra-crystalline fraction of mollusc shells have been analysed; in the case of ostrich eggshell no bleaching step was used. The molluscan racemization data reported therefore contrasts with previous work, which invariably examined D/L values from whole mollusc shells, containing both intra- and inter-crystalline material.

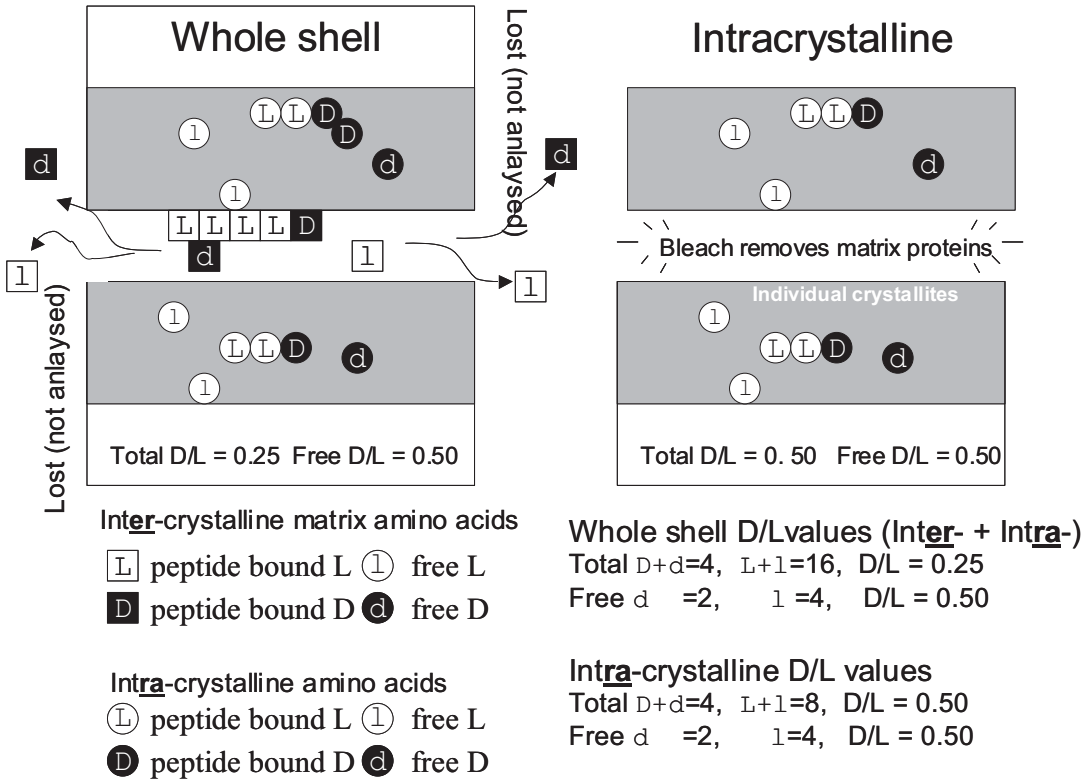

Figure 2: Schematic of intra-crystalline amino acids entrapped within carbonate crystallites. Unlike the proteins of the organic matrix between the crystallites, which leach from the shell with time, in a closed 'intra-crystalline' system the amino acids are entrapped. Thus the relationship between the DL ratios of different amino acids and between free (non-protein bound) and total (both free and originally protein-bound amino acids, released by acid hydrolysis) amino acids is predictable. Analysis of the whole shell would result in lower than expected D/L for the total fraction, due to the loss of the more highly racemized free amino acids.

This isolation of the intra-crystalline fraction is believed to provide a closed-system repository for the amino acids during the burial history of the shell. Only the amino acids within this fraction are protected from the action of external rate-affecting factors (except temperature), contamination by exogenous amino acids and leaching. Amino acids within the whole shell are not protected and can be leached out into the environment. Figure 2 shows a schematic of the intra-crystalline fraction with respect

to the whole shell. The low level of Free amino acids observed in the inter-crystalline fraction of unbleached samples (Penkman, 2005) indicates that these have been lost through diagenesis and, as these tend to be more highly racemized than the Total fraction, this loss would lead to a lower than expected D/L for the Total fraction of the whole shell.

Once a closed system inside mollusc shells has been isolated, then the kinetics of protein decomposition is much simpler to predict. In the NEaar laboratory the concept of age estimation using the extent of overall Intra-crystalline Protein Degradation (IcPD) has been devised, which links the hydrolysis, racemization and decomposition of all the amino acids isolated by this method. The concept behind the IcPD method is to combine multiple information from a single sample to derive an overall measure of the extent of diagenesis of the protein in that fossil. Similar ideas have been used before, although not in such a comprehensive way. Divergence from the normal in a plot of A/I vs Gly/Ala is thought to indicate leaching in molluscs (Murray-Wallace & Kimber, 1987). Kaufman (2000) used ratios of Asx to Glx to screen out samples with any unusual values.

Traditionally AAR studies targeted a single amino acid racemization reaction, that of L-isoleucine to D-alloisoleucine (A/I), due to the technical ease of separation and its slow rate of racemization. The approach used in this study diverges from this, as dates are derived from the analysis of multiple amino acids. Whilst racemization rates differ between individual amino acids, they should be highly correlated in a closed system. By linking together different amino acids, and then linking this to a temperature-driven model of decay that includes hydrolysis, racemization and degradation, the extent of protein degradation can be derived. The pattern of decomposition appears to differ between mollusc genera, requiring separate models for each genus or species studied.

If a closed system is isolated, it should be possible to predict the relationship between geological time and IcPD increase, using not just racemization but other measures of protein decomposition, such as total and relative concentrations. It follows from the innovations above that, assuming sampling is from an idealized closed system, the pattern of protein decomposition governs the observed racemization of (a) free amino acids and (b) the total system, (c) the percentage of free amino acids and (d) the total concentration of amino acids.

This model can also be used as a method of assessing the internal reliability of each biomineral used and to determine how closely these substrates approximate to a closed system. Subsequently palaeotemperature information can be included and estimates made of the link between degradation and absolute age in environments with fluctuating temperatures. If an accurate temperature model is used, then age estimates can be derived directly from the IcPD data, although the results presented here do not incorporate any palaeotemperature information and are presented simply as a relative dating tool.

Materials

Molluscan samples were collected and supplied by David Keen from 15 Holocene samples representing four Swale–Ure project sites. Amino acid racemization (AAR) analyses were undertaken on twelve individual *Bithynia tentaculata* opercula and three individual shells of *Valvata piscinalis*. Three opercula were analysed from four selected samples: Ripon South Section 3 (NEaar 3105–3107; see Chapter 2.6.4, Fig. 2.59); Ripon North sample1.1 (NEaar 3108–3110; see Chapter 2.6.3, Fig. 2.54 & Chapter 3.6.3); Newby Wiske 220–230 (NEaar 3123–3125; see Chapter 3.3, Fig. 3.6) and Sharow 560–570 (NEaar 3126–3128; see Chapter 3.5, Fig. 3.11). Three *Valvata piscinalis* shells (NEaar 3303–3305) were also analysed individually from the same Sharow sample (560–570) that provided the opercula.

Ripon South

Ripon South is a late Holocene site, with upper levels deposited as recently as Medieval times, although the basal deposits in the studied sections were dated by radiocarbon to *c*. 4000 BP (see Chapter 2.6 & Chapter 3.7). An OSL age estimate from the same stratum (Fig. 2.59), although of insufficient quality to be definitive, suggested an age nearer the later end of the above range (see Appendix II).

Ripon North

The sediments at Ripon North are Mid–Late Holocene in age (see Chapter 3.6), despite being slightly higher above the Ure than Terrace 2 of Howard *et al.* (2000) at their Ripon Racecourse site, from which they obtained an early Holocene (earlier than 9 ka BP) radiocarbon date (see Chapter 3.7). The lower clastic sediments at Ripon North contain *Theodoxus fluviatilis* (see Chapter 3.6), which first appeared in Britain in the Holocene between 7 and 6 ka BP. Overlying finer grained organic sediments had started accumulating by *c*.3900 BP, based on a ^{14}C date, whereas a later date of *c*.2325 BP coincides with the first appearance of cereal-type pollen within the

sequence. The opercula came from the fully clastic sediments and are thus likely to be older than the earlier ^{14}C date but later than the appearance of *T. fluviatilis*.

Newby Wiske

The Newby Wiske yielded a pollen profile with an almost complete sequence from Lateglacial to mid-Neolithic times. The selected opercula came from a sample at 220–230, from the uppermost part of the marl unit. The range of other age indicators from the site would place this level at an age of about 8800 BP (see Chapter 3.3; Fig. 3.7).

Sharow Mires

The Sharow site preserves a long sequence of Late Holocene deposits beneath the floor of an abandoned channel. These organic sediments are presumed to have accumulated after the channel was abandoned by the Ure, which, from the lowest radiocarbon date, was around 4000–4500 years ago. The sample from 560–570 depth, which yielded the analysed opercula and shells, falls between two radiocarbon dates that overlap at one standard deviation and indicate an age of 2400–2480 years (Fig. 3.12).

For further details of the sites and their faunas see Chapters 2 and 3.

Sample Preparation

Shells were examined under a low powered microscope and any adhering sediment removed. The shell samples were then sonicated and rinsed several times in HPLC-grade water. The shells were then crushed to <100 μm. Only bleached samples were analysed.

Bleaching

50 μl of 12% solution of sodium hypochlorite at room temperature was added to each milligram of powdered sample and the caps retightened. The powders were bleached for 48 hours with a shake at 24 hours. The bleach was pipetted off and the powders were then rinsed five times in HPLC-grade water with a final rinse in HPLC-grade methanol (MeOH) to destroy any residual oxidant (by reaction with the MeOH). The bulk of the MeOH was pippetted off and the remainder left to evaporate to dryness.

Hydrolysis

Protein bound amino acids are released by adding an excess of 7 M HCl to the bleached powder and hydrolysing at 110^{o}C for 24 hours (H*), resulting in the Total Hydrolysable amino acid fraction.

20 µl per milligram of sample of 7 M Hydrochloric Acid (HCl) was added to each Hydrolysis ('Hyd', H*) sample in sterile 2 ml glass vials, were flushed with nitrogen for 20 seconds to prevent oxidation of the amino acids, and were then placed in an oven at 110°C for 24 hours. After 10 minutes in the oven, the caps of the 2 ml vials were re-tightened to prevent the escape of vapour.

After 24 hours, the samples were dried in a centrifugal evaporator overnight.

Demineralisation

Free amino-acid samples ('Free', F) were demineralised in cold 2 M HCl, which dissolves the carbonate but minimizes the hydrolysis of peptide bonds, and then dried in the centrifugal evaporator overnight.

Rehydration

When completely dry, samples were rehydrated with 10 µl per mg of Rehydration Fluid: a solution containing 0.01 mM HCl, 0.01 mM L-homo arginine internal standard, and 0.77 mM sodium azide at a pH of 2. Each vial was vortexed for 20 seconds to ensure complete dissolution and checked visually for undissolved particles.

Approximately 20 µl of rehydrated sample was then placed in a sterile, labelled 2 ml autosampler vial containing a glass insert, capped and then placed on the autosampler tray of the HPLC.

For each set of subsamples a blank vial was included at each stage to account for any background interference from the bleach, acid, or rehydration fluid added to the samples.

Analysis of Free and Hydrolysed Amino Acids

Amino acid enantiomers were separated by Reverse Phase High Pressure Liquid Chromatography (RP-HPLC). NEaar uses a modified method of Kaufman and Manley (1998), using an automated RP-HPLC system. This method achieves separation and detection of L and D isomers in the sub-picomole range.

Samples (2 µl) were derivitized with 2.2 µl *o*-phthaldialdehyde and thiol *N*-isobutyryl-L-cysteine automatically prior to injection. The resulting diastereomeric derivatives were then separated on Hypersil C_{18} BDS column (sphere d. 5 µm; 250 x 3 mm) using a linear gradient of a sodium acetate buffer (23 mM sodium acetate, 1.3 mM Na_2EDTA; pH6), methanol, and acetonitrile on an integrated HP1100 liquid chromatograph (Hewlett-Packard, USA).

Individual amino acids are separated on a non-polar stationary phase according to their varied retention times: a function of their mass, structure, and hydrophobicity. A fluorescence detector is used to determine the concentrations of each amino acid and record them as separate peaks on a chromatogram. A gradient elution programme was used to keep the retention time to below 120 minutes.

The fluorescence intensity of derivitized amino acids was measured (Ex = 230 nm, Em = 445 nm) in each sample and normalized to the internal standard. All samples and blank extracts that had been subjected to identical preparation procedures were run in triplicate. Quantification of individual amino acids was achieved by comparison with the standard amino acid mixture.

External standards containing a variety of D- and L- amino acids, allowing calibration with the analyte samples, were analysed at the beginning and end of every run, and one standard was analysed every ten samples. Blanks were randomly interspersed amongst the standards.

The L and D isomers of 10 amino acids were routinely analysed. During preparative hydrolysis both asparagine and glutamine undergo rapid irreversible deamination to aspartic acid and glutamic acid respectively (Hill, 1965). It is therefore not possible to distinguish between the acidic amino acids and their derivatives and they are reported together as Asx and Glx.

Results and Discussion

In total 60 analyses were conducted, all of which were on bleached samples. As anticipated, bleaching reduced the yields of amino acids and also increased reproducibility.

On the basis of the relative D/L values and concentrations (Supplement 4) the amino acid data from the opercula from Ripon South, Ripon North and Newby Wiske, when

compared with unpublished values from Quaternary sites within the UK, are consistent with an age assignment within the Holocene.

The data obtained from Asx, Glx, serine, alanine and valine is discussed in detail below.

Aspartic acid / Asparagine (Asx)

Asx is one of the fastest racemizing of the amino acids discussed here (due to the fact that it can racemize whilst still peptide bound; Collins *et al*., 1999). The values of Asx D/L for the Free samples from Ripon South are the lowest within this study (Fig. 3), although the very low Free concentrations make the determination of the D/L difficult (Fig. 4). The Free Asx D/L of Ripon North is higher than that of Ripon South, with slightly higher concentrations in the Free form. This indicates that these opercula are slightly older than those from Ripon South, as more protein hydrolysis has occurred. However, the extent of racemization in the Hyd samples for these two sites is very similar, indicating that there is not a huge difference in age between these

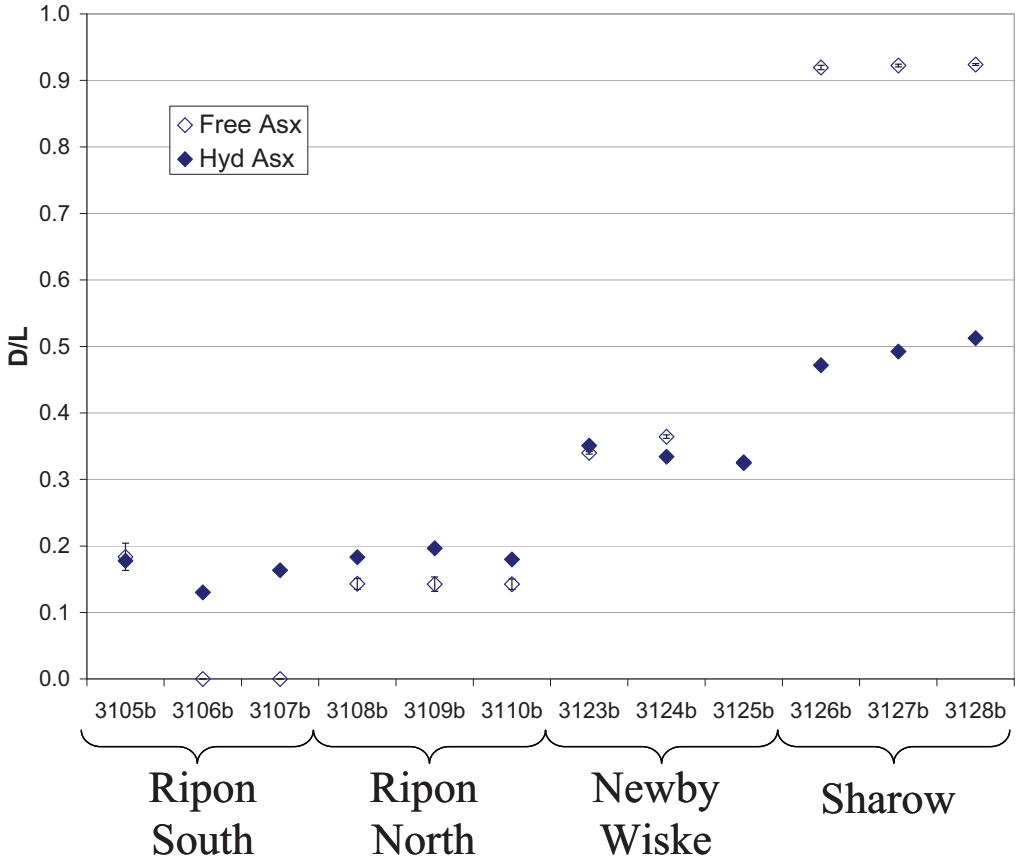

Figure 3: Free (open symbols) and Hydrolysed (closed symbols) D/L values for Asx in *Bithynia tentaculata* opercula. Error bars represent one standard deviation about the mean for the duplicate analyses.

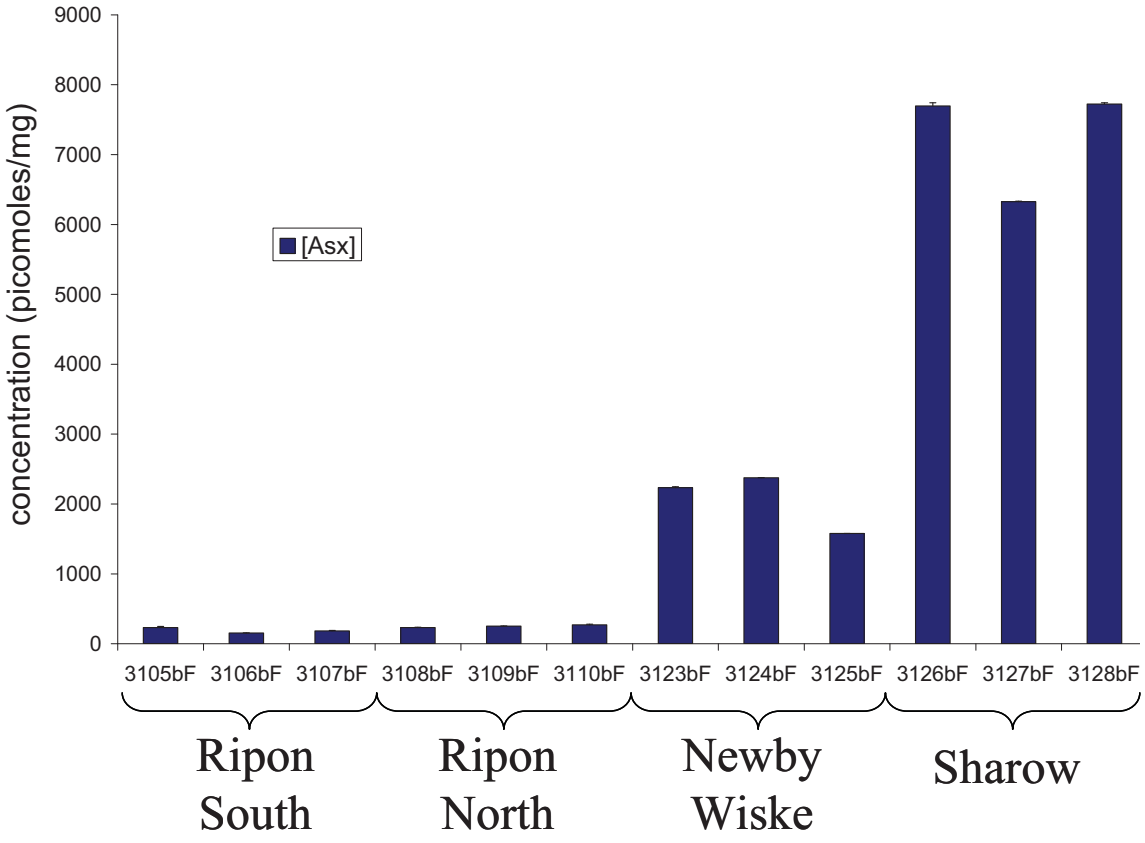

Figure 4: Free Asx concentrations (in picomoles/mg) in *Bithynia tentaculata* opercula. Error bars represent one standard deviation about the mean for the duplicate analyses.

two sites. There is a clear increase in the extent of racemization in the Newby Wiske samples, in both the Free and Hyd fractions, with a significant increase also seen in the concentration of Asx in the Free fraction. Clearly there has been more protein breakdown in the Newby Wiske samples.

The Free Asx values for Sharow are extremely high, similar to values obtained from sites of Cromerian age. However, the values obtained from the Hyd fraction are lower, although not as low as Holocene levels. The concentration of Free Asx is very high. When the Free to Hyd graph is plotted (Fig. 5), the Sharow data falls significantly off the expected line. This suggests that these samples are compromised.

When compared to other Holocene samples analysed at NEaar (Fig. 5), the Ripon South and Ripon North samples have lower values that those obtained from Enfield Lock and Quidenham Mere. The Newby Wiske samples fall higher than those from Quidenham Mere and Enfield Lock. The Enfield Lock opercula come from just below a radiocarbon date of 6650 ± 50 BP (Chambers *et al.*, 1996) whilst the Quidenham Mere samples have been radiocarbon dated to ~ 5000 BP (R.C. Preece, pers. comm.). The extent of

racemization in the Newby Wiske samples is less than that observed from the earliest samples from Star Carr (245-250) which lie below a radiocarbon date of 7640 ± 85 BP.

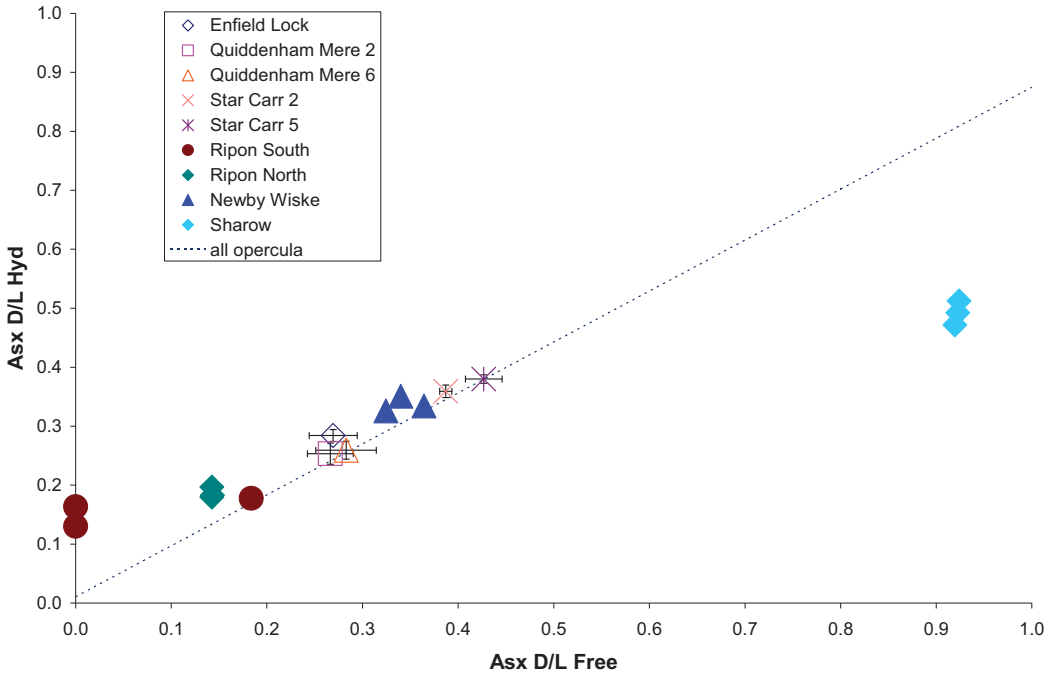

Figure 5: D/L Hyd vs D/L Free for Asx in *Bithynia tentaculata* opercula, compared to other Holocene samples and the trend-line observed for fossil samples (in black). Note the abnormal DL ratios for Sharow. The error bars represent two standard deviations about the mean for multiple samples. Two of three samples from Ripon South had levels of free amino acids so low that it was not possible to determine D/L Asx.

Glutamic Acid/Glutamine (Glx)

Glx is one of the slower racemizing amino acids discussed here and so the level of resolution at these young sites is less than that seen with faster racemizing amino acids such as Asx. It is noteworthy that Glx has a slightly unusual pattern of racemization in the free form, due to the formation of a lactam (see Walton, 1998). This results in difficulties in measuring Glx in the Free form, as the lactam cannot be derivitized and is therefore unavailable for analysis.

The values of Glx D/L for the Free samples from Ripon South and Ripon North are the lowest (Fig. 6), as the concentration of D-Glx in these samples was below the level of resolution of this technique (Fig. 7). The Free D/L in the samples from Newby Wiske are all higher, with concomitant increased concentrations. More protein breakdown has occurred in the Newby Wiske samples, indicating that it is older than the Ripon sites.

The Hydrolysed D/L values are very similar across these three sites, although the samples from Newby Wiske have slightly elevated values over the Ripon sites.

The Free Glx values for Sharow are extremely high, similar to values obtained from sites of Cromerian age. However, the values obtained from the Hyd fraction are lower, although again not as low as Holocene levels. The concentration of Free Glx is similar to that from the samples at Newby Wiske, but it is likely that this is due to the difficulties of analysis of Free Glx due to lactam formation, rather than being a true representation of the concentration of Free Glx.

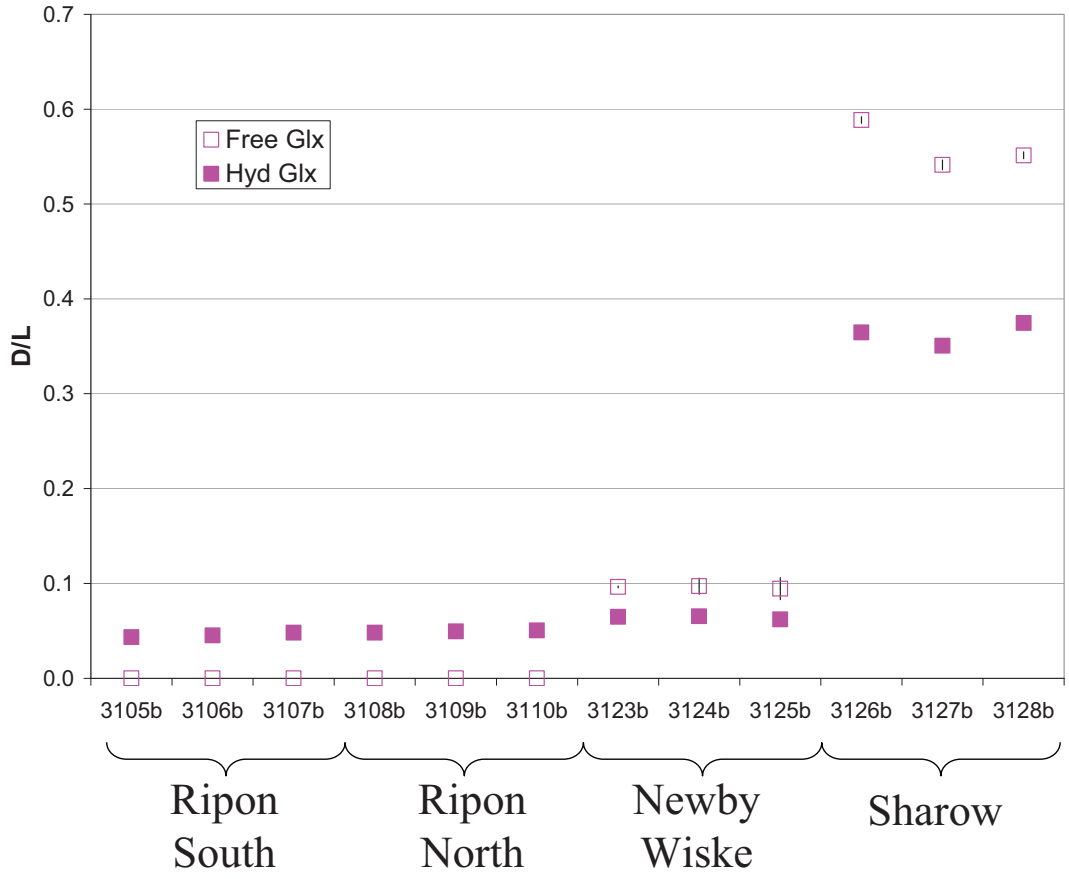

Figure 6: D/L Free (open symbols) and D/L Hydrolysed (closed symbols) for Glx in *Bithynia tentaculata* opercula. Error bars represent one standard deviation about the mean for the duplicate analyses.

Serine (Ser)

Serine is one of the most unstable amino acids, with fast rates of racemisation and decomposition. It is therefore very useful for discriminating between sites at younger timescales as in this study.

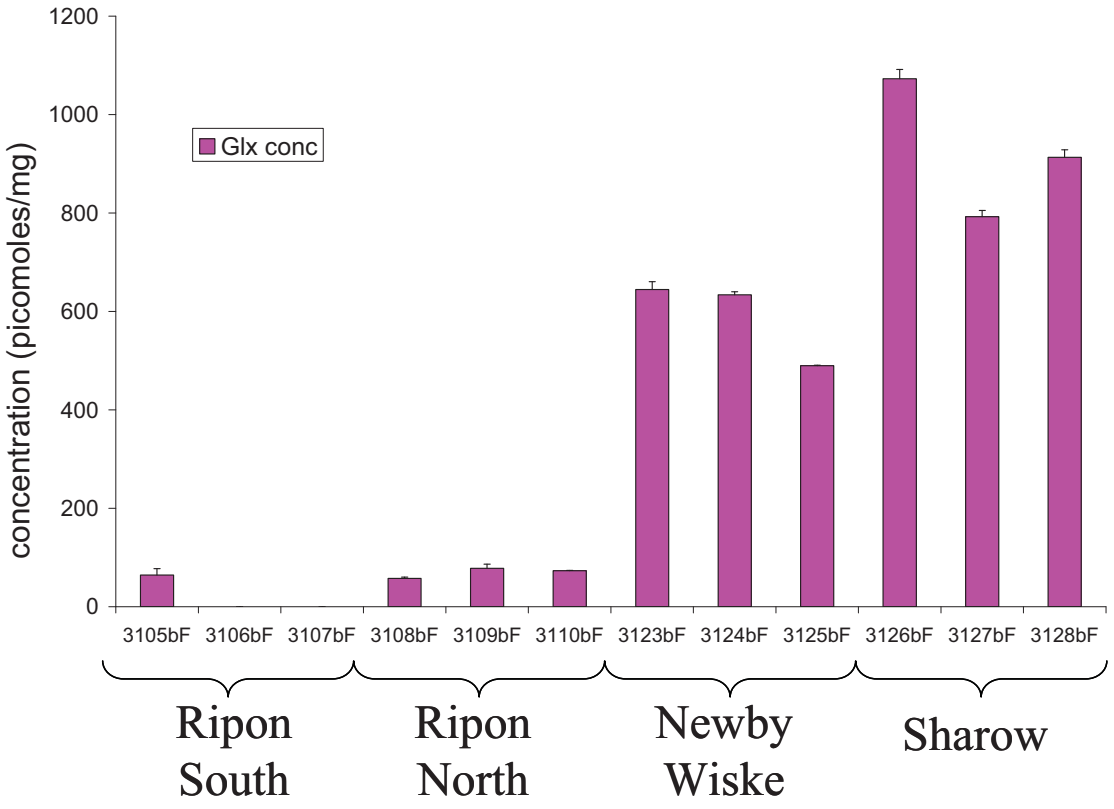

Figure 7: Free Glx concentrations (in picomoles/mg) in *Bithynia tentaculata* opercula. Error bars represent one standard deviation about the mean for the duplicate analyses.

The values of Ser D/L for the Free samples from Ripon South are the lowest (Fig. 8), although in two of the samples the concentration of D-Ser was below the level of resolution of this technique (Fig. 9). The D/L Ser of the Ripon North samples are higher, with increased concentrations. The Free D/L in the samples from Newby Wiske are all significantly higher, with concomitant increased concentrations. More protein breakdown has occurred in the Newby Wiske samples, indicating that this site is older than the Ripon sites.

The Hydrolysed D/L values show an increase from Ripon South with the lowest, to slightly higher values from Ripon North and the highest values from Newby Wiske. Interestingly the Ser values for Sharow are not as extreme as those seen in the other amino acids. The Free Ser D/L is similar to that seen in the Newby Wiske samples, although the Free concentrations are the lowest in all the samples analysed. The Hyd D/L values fall between those from Ripon North and Newby Wiske. The concentration of Ser in the Hyd fraction is also very low (Fig. 10), indicating significant Ser decomposition. When the Free to Hyd graph is plotted (Fig. 11), the Sharow data does appear to have

lower than expected Hyd values given the extent of racemization seen in the Free fraction. This suggests that these samples are compromised.

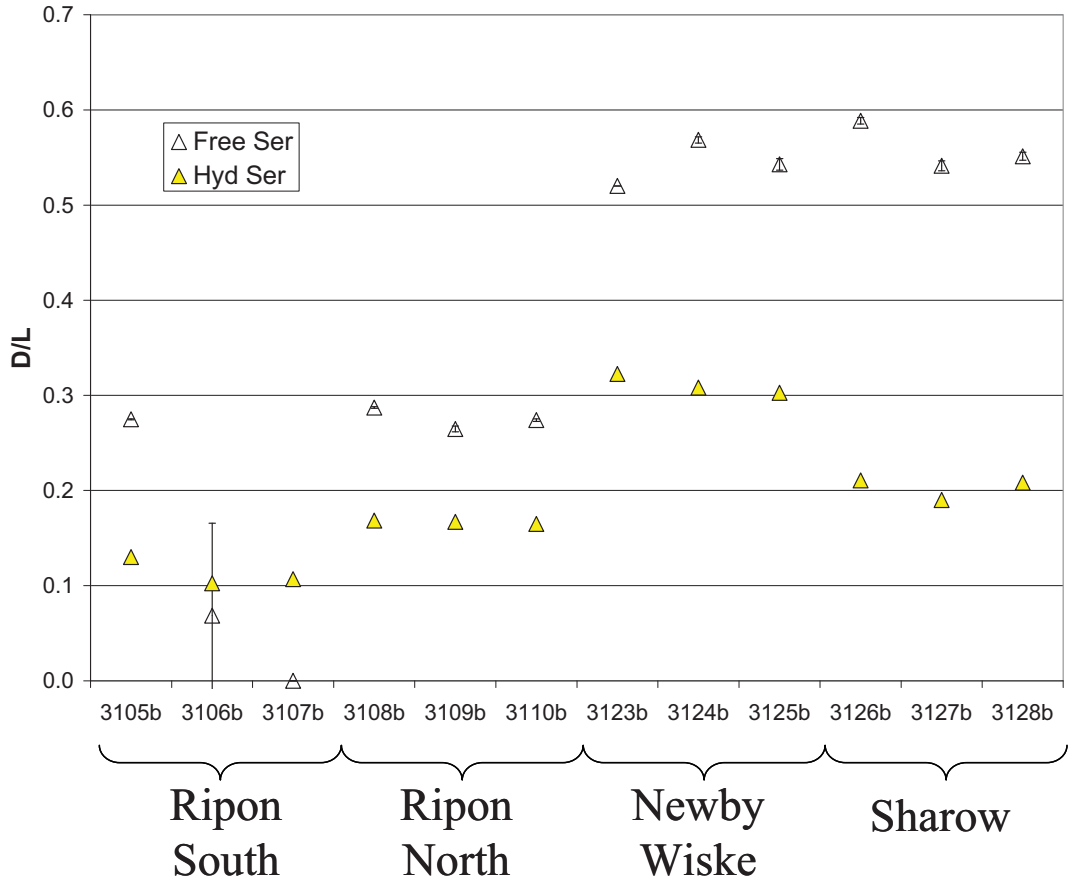

Figure 8: Free (open symbols) and Hydrolysed (closed symbols) D/L values for Ser in *Bithynia tentaculata* opercula. Error bars represent one standard deviation about the mean for the duplicate analyses.

When compared to other Holocene samples analysed at NEaar (Fig. 11), the Ripon South and Ripon North samples have lower values than those obtained from Enfield Lock and Quidenham Mere. Newby Wiske samples fall higher than those from Quidenham Mere and Enfield Lock. The Enfield Lock opercula come from just below a radiocarbon date of 6650 ± 50 BP (Chambers *et al.*, 1996) whilst the Quidenham Mere 2 samples have been radiocarbon dated to ~ 5000 BP. The extent of racemization in the Newby Wiske samples is less than that observed from Star Carr.

Alanine

Alanine (Ala) is a hydrophobic amino acid, whose concentration is partly contributed from the decomposition of other amino acids (notably Serine). The results for Ala are broadly similar to that seen in the other amino acids, although the level of resolution is less due to the slower rates of racemisation. The alanine data supports the interpretation

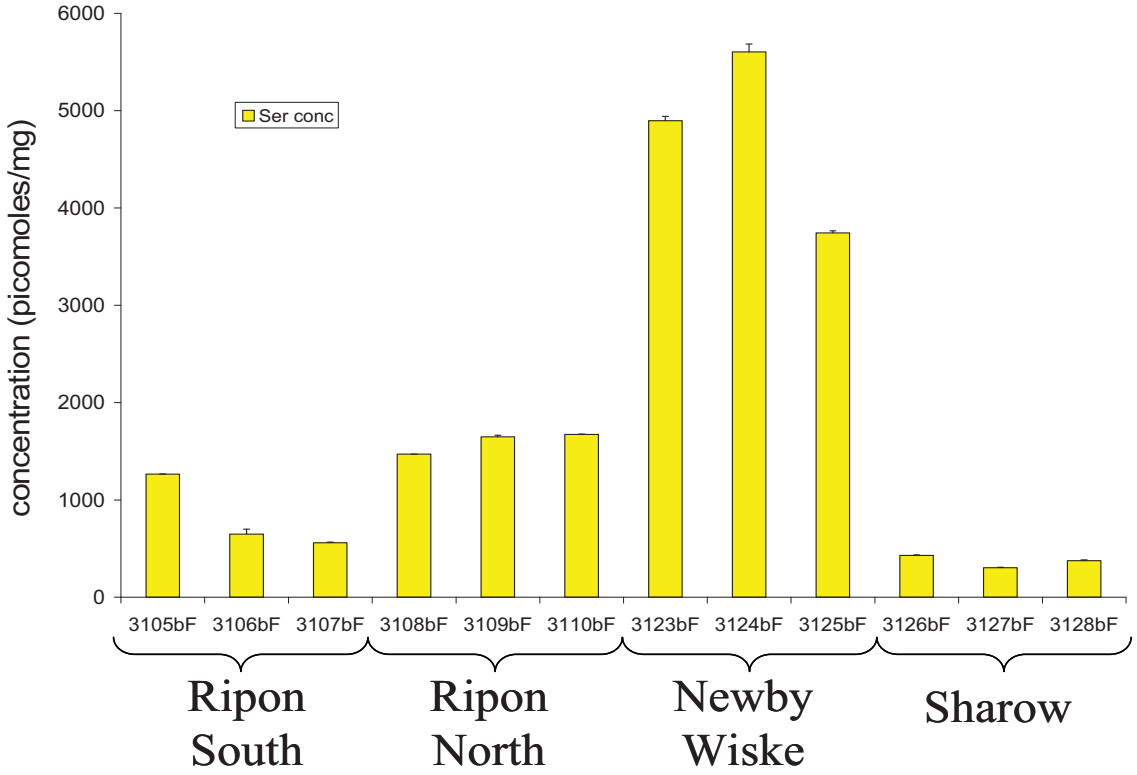

Figure 9: Free Ser concentrations (in picomoles/mg) in *Bithynia tentaculata* opercula. Error bars represent one standard deviation about the mean for the duplicate analyses.

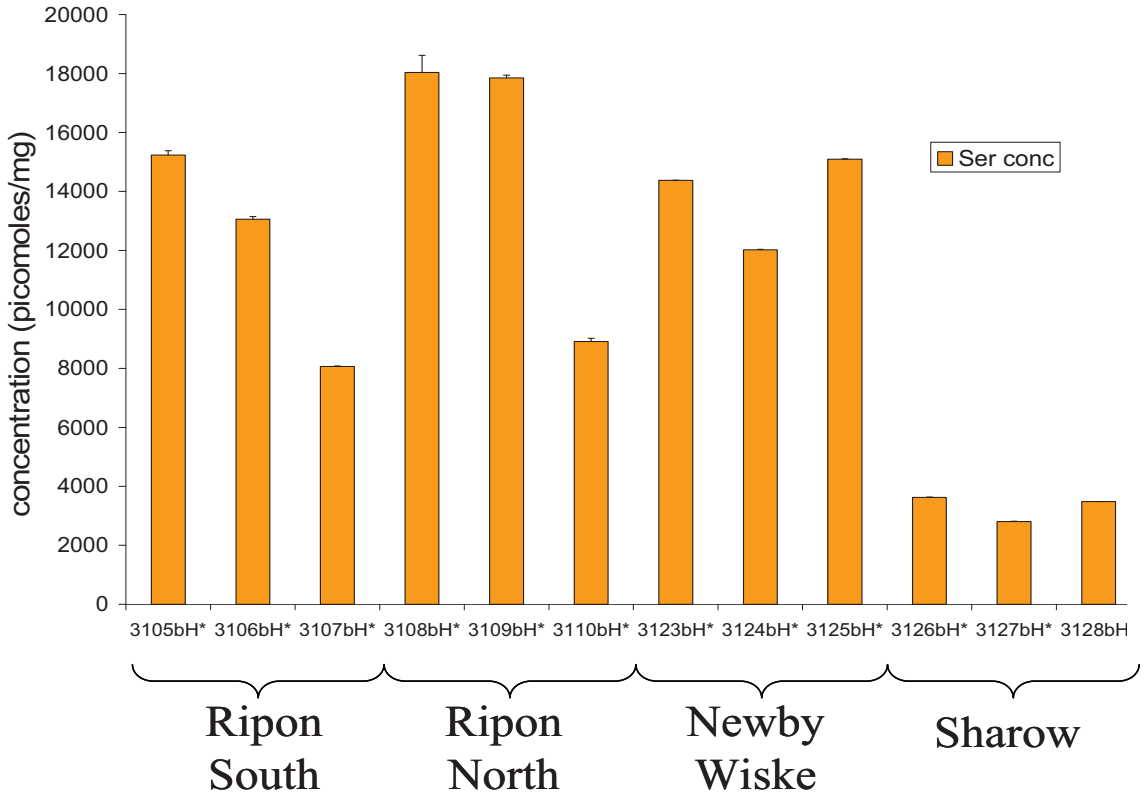

Figure 10: Hydrolysed (Total) Ser concentrations (in picomoles/mg) in *Bithynia tentaculata* opercula. Error bars represent one standard deviation about the mean for the duplicate analyses.

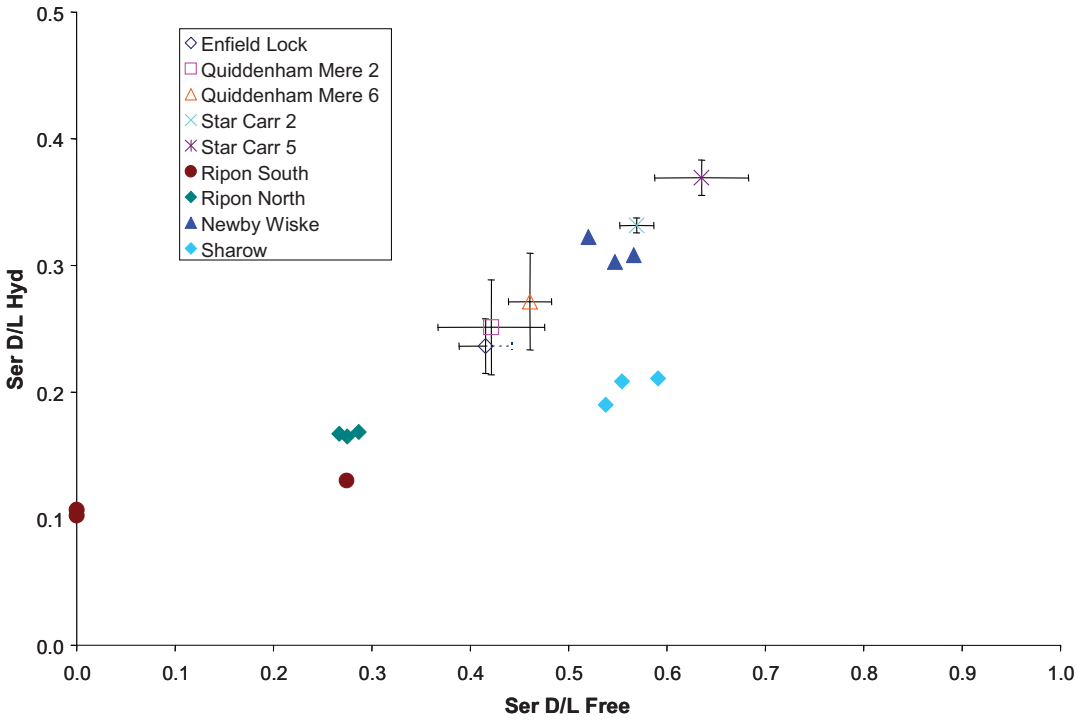

Figure 11: D/L Hyd vs D/L Free for Ser in *Bithynia tentaculata* opercula, compared to other Holocene samples. Note the abnormal DL ratios for Sharow. The error bars represent two standard deviations about the mean for multiple samples.

that Ripon South and Ripon North are of similar age, with Ripon South likely to be slightly younger, and Newby Wiske being older.

The values of Ala D/L for the Free samples from Ripon South and Ripon North are the lowest (Fig. 12), with similar low concentrations to that of Ripon North (Fig. 13). The Free D/L in the samples from Newby Wiske are all higher, with increased concentrations. More protein breakdown has occurred in the Newby Wiske samples, indicating that this site is older than the Ripon sites.

The Hydrolysed D/L values are very similar across these three sites, although the samples from Newby Wiske have slightly elevated values over the Ripon sites. The Free Ala values for Sharow are extremely high, similar to values obtained from sites of Cromerian age. However, the values obtained from the Hyd fraction are lower, although again not as low as Holocene levels. The concentration of Free Ala is very high, indicating high levels of protein hydrolysis. When the Free to Hyd graph is plotted, the Sharow data falls significantly off the expected line. This suggests that these samples are compromised.

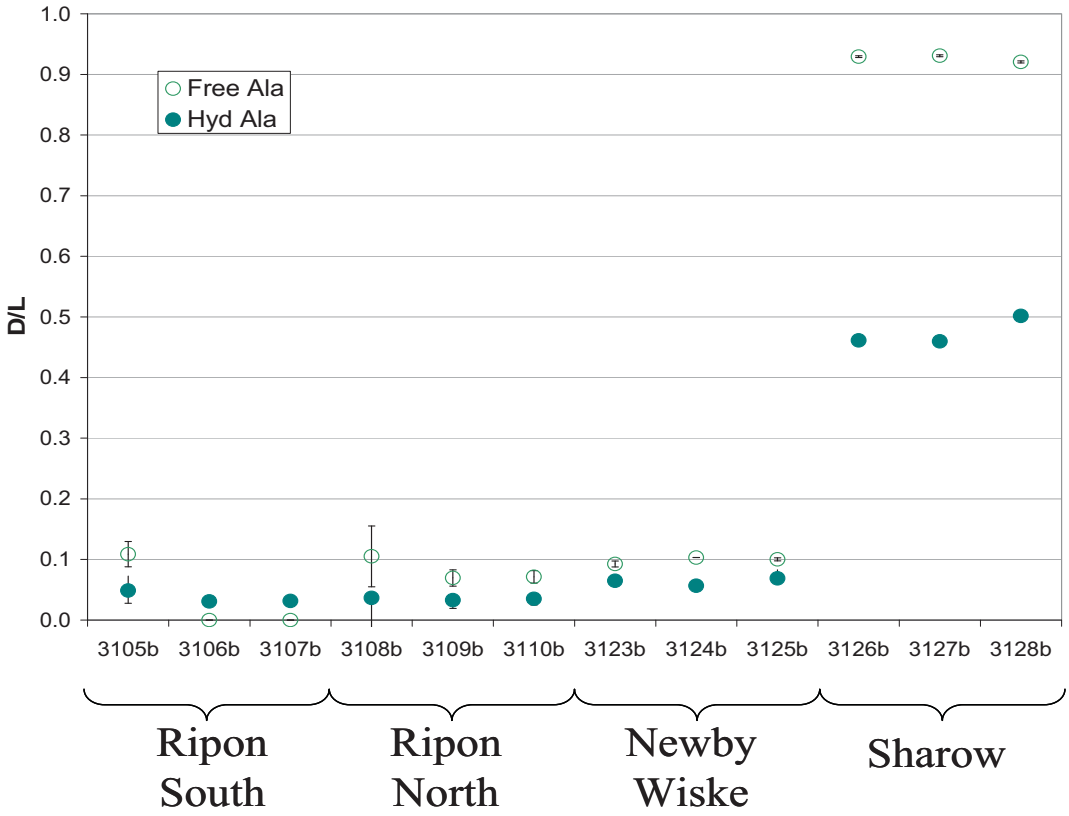

Figure 12: Free (open symbols) and Hydrolysed (closed symbols) D/L for Ala in *Bithynia tentaculata* opercula. Error bars represent one standard deviation about the mean for the duplicate analyses.

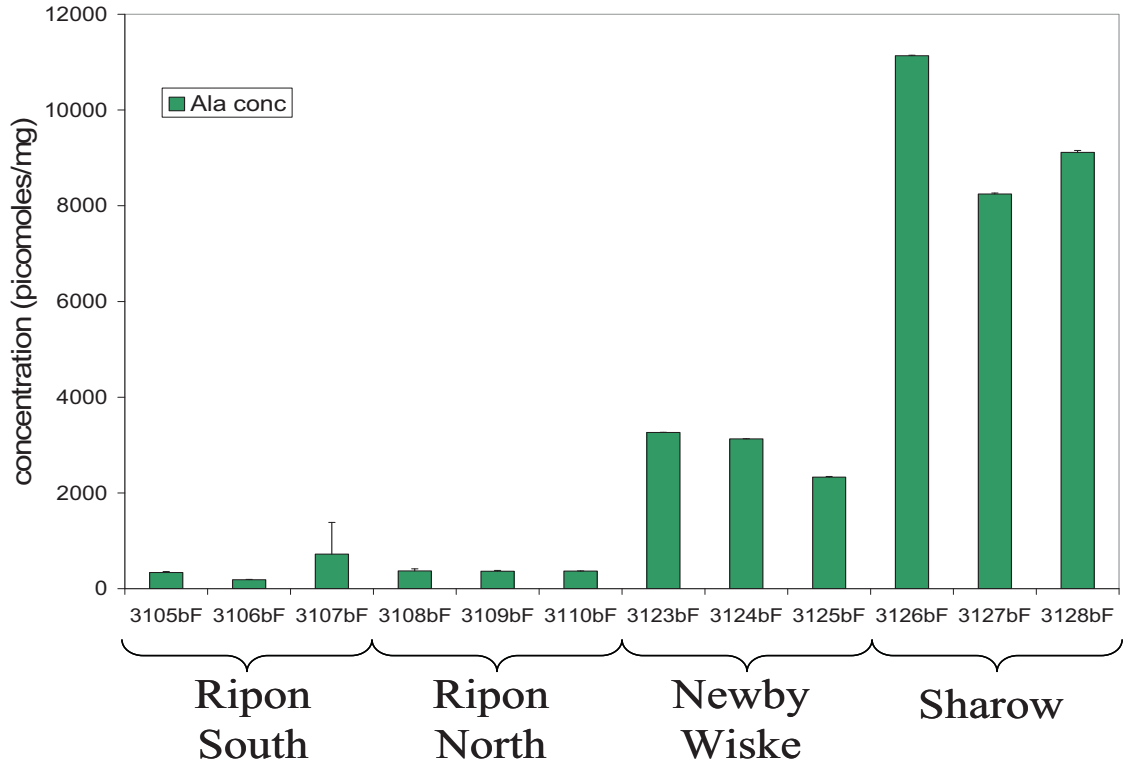

Figure 13: Free Ala concentrations (in picomoles/mg) in *Bithynia tentaculata* opercula. Error bars represent one standard deviation about the mean for the duplicate analyses.

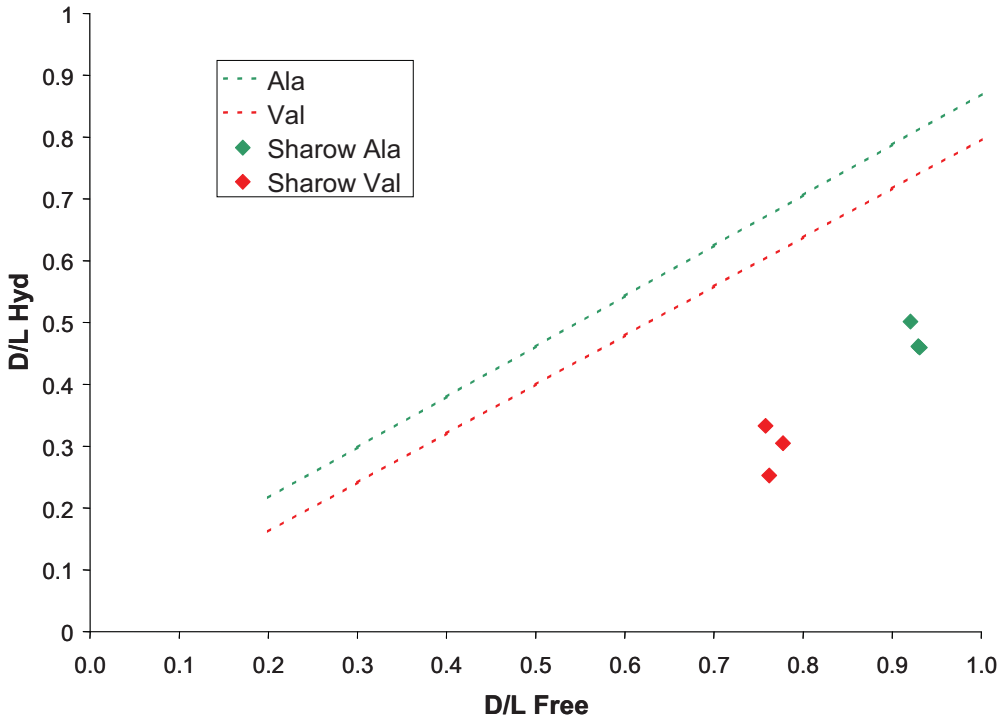

Figure 14: D/L Hyd vs D/L Free for Ala and Val in *Bithynia tentaculata* opercula from Sharow, compared to other Quaternary samples.

Valine (Val)

Valine has extremely low rates of racemisation, and is therefore less useful for age discrimination within Holocene material.

The Val D/L in the Free fraction does not strongly discriminate between the sites (except for Sharow). This is partly due to the slow rate of racemization, but also because the concentration of the Free Val in the Ripon sites is so low that the errors in determining the D/L values are extremely large (Fig. 15). However, the concentration of Free Val is elevated in the Newby Wiske samples compared to the Ripon sites, indicating increased protein breakdown (Fig. 16). In the Hyd fraction the D/L of Newby Wiske is very slightly higher than that seen in the Ripon material.

The most notable aspects of the Val data is that the same problematic samples from Sharow identified for Asx, Glx, Ser and Ala are also seen with Val, further confirming that these samples are compromised. The Free Val values for Sharow are extremely high, similar to values obtained from sites of Cromerian age. However, the values obtained from the Hyd fraction are lower, although again not as low as Holocene levels. The concentration of Free Val is very high, indicating high levels of protein hydrolysis. When the Free to Hyd graph is plotted, the Sharow data falls significantly off the expected line (Fig. 14). This suggests that these samples are compromised.

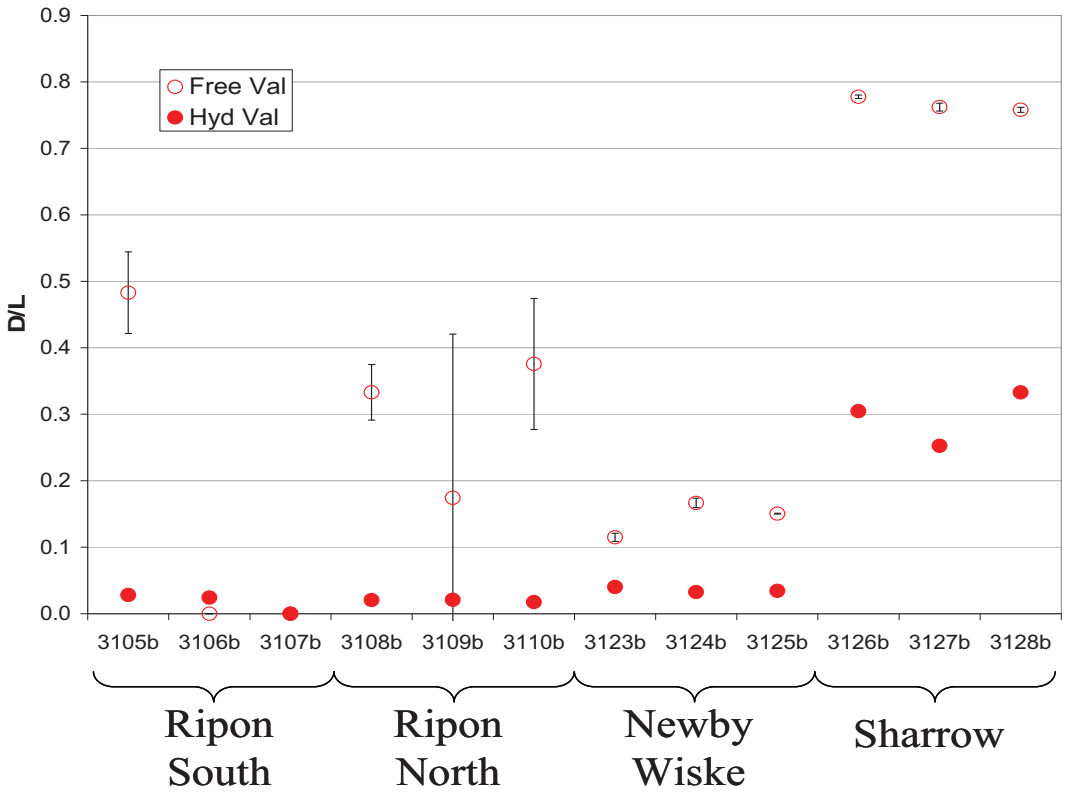

Figure 15: Free (open symbols) and Hydrolysed (closed symbols) for Val in *Bithynia tentaculata* opercula.

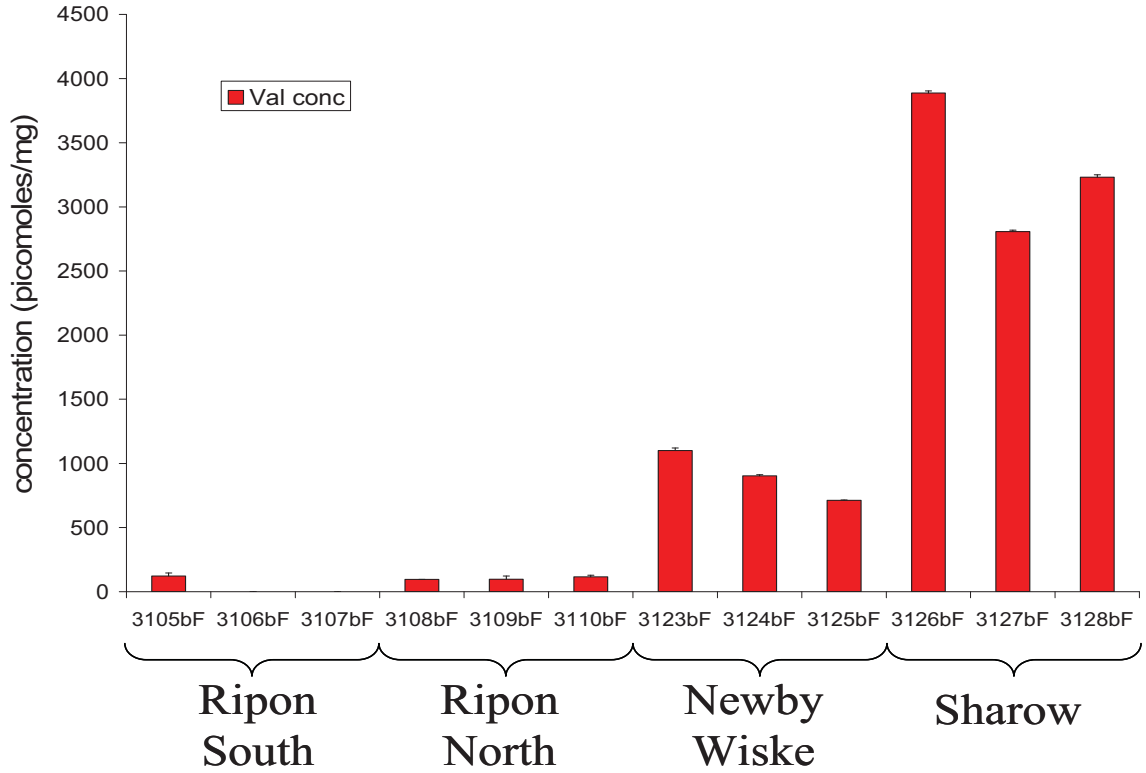

Figure 16: Free Val concentrations (in picomoles/mg) in *Bithynia tentaculata* opercula. Error bars represent one standard deviation about the mean for the duplicate analyses.

[Serine]/[Alanine]

The ratio of the concentrations of Serine and Alanine provides a useful tool for age estimation. Serine is a very unstable amino acid, and it can degrade via dehydration into alanine (Bada *et al.,* 1978). As the protein within a sample breaks down, the concentration of serine will decrease with an increase in the concentration of alanine, thus the [Ser]/[Ala] value will decrease with increasing time.

The [Ser]/[Ala] of the Ripon samples is very similar in both the Free and the Hyd fractions, but a decrease is observed in the Newby Wiske material, indicating that these samples are older (Fig. 17). The large errors observed in NEaar 1307 are due to the low concentrations involved. The Sharow samples have very low values of [Ser]/[Ala] in both the Free and Hyd fractions.

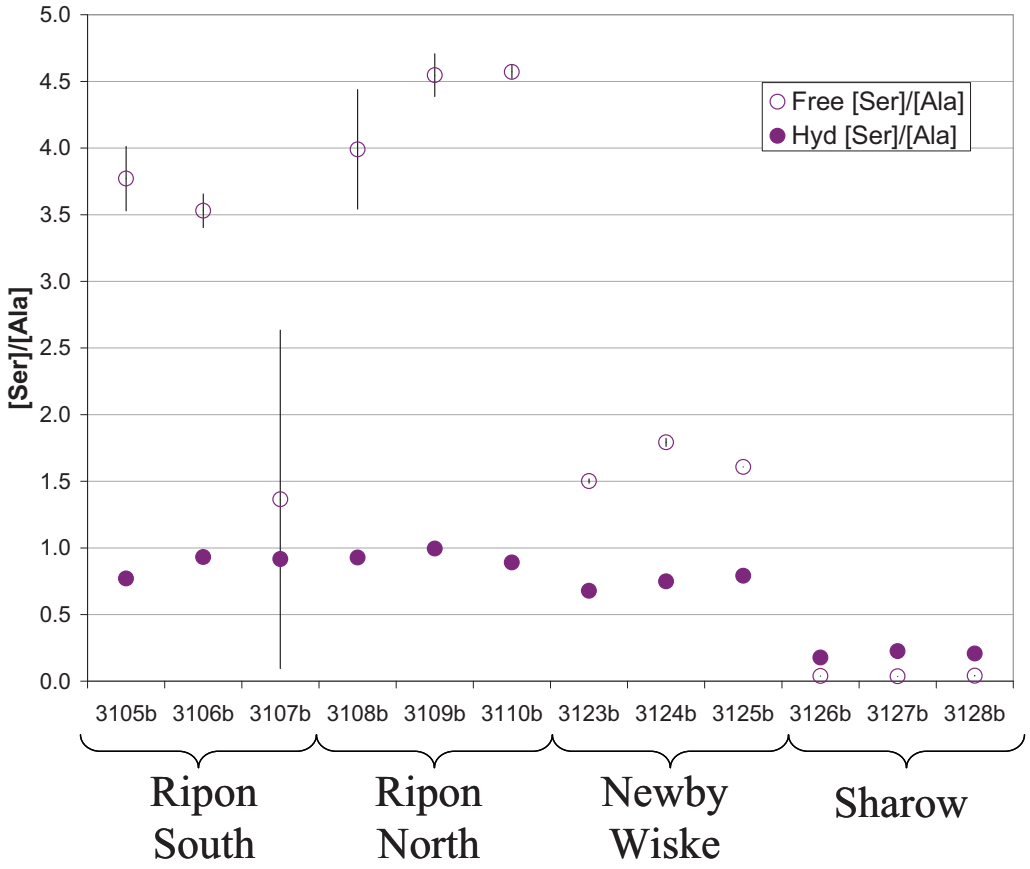

Figure 17: Free (open symbols) and Hydrolysed (closed symbols) for [Ser]/[Ala] in *Bithynia tentaculata* opercula. Error bars represent one standard deviation about the mean for the duplicate analyses.

Valvata piscinalis shell results

Given the unexpected results obtained from the *Bithynia tentaculata* opercula from Sharow, further analyses were undertaken on *Valvata piscinalis* shell material from the same horizon. Amino acid racemisation is governed by sequence and conformation. Whilst developing the research into closed-system protein degradation it became clear that the reaction rates were species-specific, even in the intra-crystalline fraction (Penkman *et al*., 2007). This necessitates the comparison of amino acid data only within a single species, meaning that the *Valvata piscinalis* data cannot be directly compared to the data from the other sites, as a different material was used. However, a large database of amino acid data from fossil *Valvata piscinalis* has been developed (Penkman, 2005; Penkman *et al*., 2007) to which the Sharow samples can be compared. The amino acid data obtained from these shells showed extremely high levels of racemization and protein degradation (Fig. 18), just as seen in the opercula. One sample, NEaar 3304, has lower D/L values in the Hydrolysed fraction.

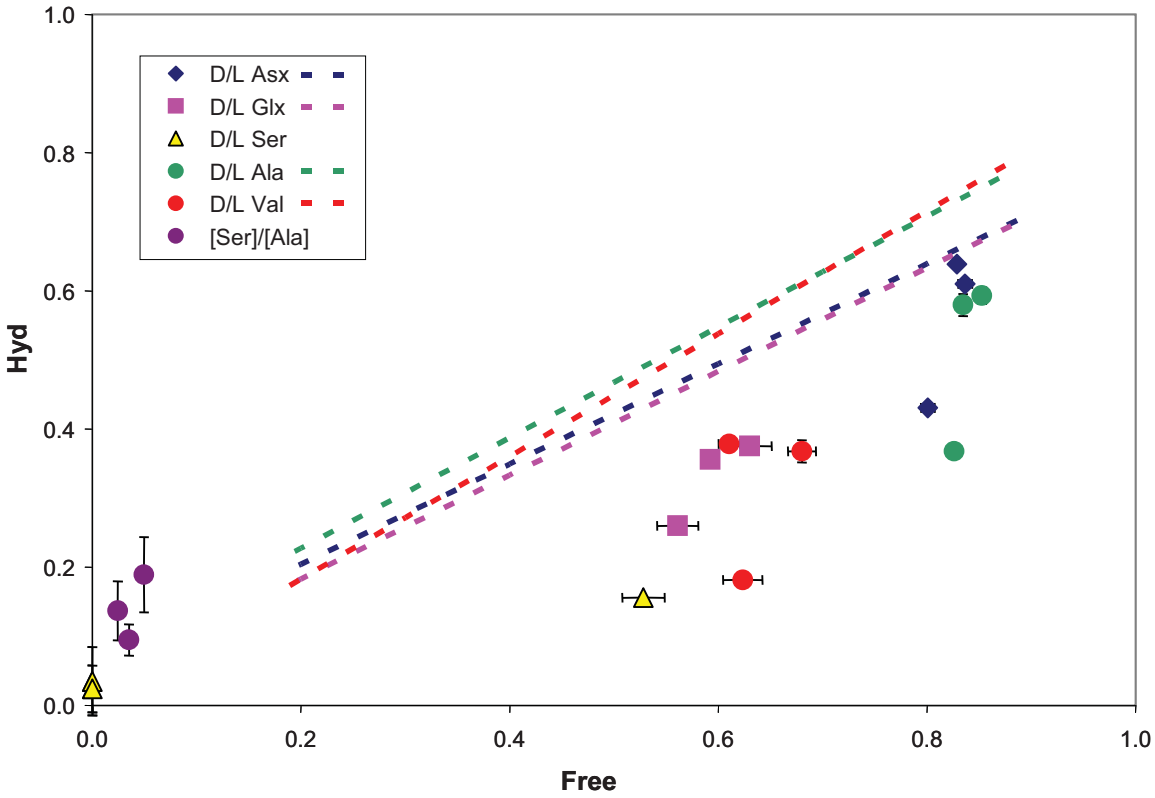

Figure 18: Hyd vs Free for D/L of Asx, Glx, Ser, Ala, Val and [Ser]/[Ala] in *Valvata piscinalis* shell, compared to the trendlines observed for fossil samples for D/L of Asx, Glx, Ala and Val. The DL ratios for Sharow are abnormal. The error bars represent one standard deviation about the mean for duplicate analyses. Whilst the Free values are similar for each sample, in the Hyd fraction NEaar 3304bH* has low ratios.

Whilst the extent of protein degradation is too high for that expected from Holocene samples, the Hyd ratios are too low given the extent of protein degradation in the Free fraction. This divergence from the trend observed for other *Valvata piscinalis* shells can clearly be seen (Fig. 18), and shows that the intra-crystalline fraction has been compromised. Therefore no age estimation can be made from these samples.

Discussion

Sharow samples

The amino acid data obtained from the Sharow samples, both in the *Valvata piscinalis* shell and the *Bithynia tentaculata* opercula, showed very high levels of amino acid racemization and protein degradation. This extent of protein breakdown is not consistent with that expected from Holocene samples. It is possible that these samples have been reworked from much older deposits. However, there are significant indications that the integrity of the closed system of intra-crystalline protein has been compromised in some way.

If the sample had been contaminated by microbial action or undergone recrystallisation during its burial history, then the Free to Hyd values of one or more of the amino acids will not match. When the Hyd ratios are compared to the Free ratios from the same sample, they fall clearly well out of the range of any operculum or shell yet analysed (Figs 5, 11, 14 & 18). If the amino acids are contained within a closed system the relationship between the Free and the Hyd would be highly correlated, as evidenced by the tight clustering of Free to Hyd ratios observed for the other opercula (Penkman, 2005; Preece & Penkman, 2005). That these samples plot well away from these general trends is an indication that post-mortem protein contamination or leaching has occurred.

In the case of the *Bithynia tentaculata* opercula and the *Valvata piscinalis* shells from Sharow, the original amino acid composition has clearly been compromised and no age assignment is possible for these samples. The tight correlation of the Free to Hyd ratios allows this alteration to be recognised, and therefore data from the opercula to be rejected. Analysis of just one of these fractions could lead to an erroneous age assignment, without recognition of the composition discrepancies. It is therefore essential that any amino acid analysis is conducted on both the Free and the Hyd fractions from the same sample, and that age correlations using amino acids are not made on the basis of single samples.

The Free amino acid levels from the Sharow samples indicate far more protein decomposition than the Hyd amino acids from the SAME shell. One possible

explanation for high Free and low Hyd values is corrosion. One possible explanation for high Free and low Hyd values is corrosion. If dissolution was the cause then the Free values would be as high or higher than in a reliable sample, whilst the Hyd values would be depressed, as observed in this material. That all samples from this horizon, comprising two different biomineral types, have been compromised indicates that this is due to an as-yet-unknown factor in the burial environment.

Comparison with other Holocene sites

Five other Holocene opercula samples with known ages can be used to tentatively constrain the ages of the Swale-Ure samples. *Bithynia tentaculata* opercula have been analysed from two depths from a core taken in 2005 at Quidenham Mere (250–260 cm and 640–650 cm); from Enfield Lock (3, 10–15cm) and from two horizons from Star Carr (245–250 cm and 524–528 cm).

The samples from Quidenham Mere come from a core adjacent to one that has been radiocarbon dated. Sample 2 comes from the 250–260 cm level and is about 5000 yr BP (R. Preece, pers.comm). Sample 6 comes from the 640–650 cm level and is harder to date, but is older than sample 2, and younger than 9250 yr BP.
The opercula from Enfield Lock come from just below the radiocarbon date of 6650 ± 50 BP (Chambers *et al*., 1996).

The samples from Star Carr come from the pollen core taken from the new palaeoecological investigations undertaken by Petra Dark (Mellars, 1998). Sample 2 comes from the 245-250 cm level from marl immediately below the switch from marl to organic lake mud. The base of the mud has been dated to 7640 ± 85 BP, with the opercula likely to be only marginally earlier unless there is a hiatus. Sample 5 comes from the 524–528 cm level, representing a late-glacial interstadial woodland recession/cooling phase, estimated to have been deposited between C. 11,300–11,400 BP.

The amino acid data from the Swale-Ure opercula enable relative age determinations to be made for this material, assuming similar temperature histories. The faster-racemising and decomposing amino acids allow a better resolution with sites of this age and so the age comparisons are based on the racemisation of Asx (Fig. 6), Ser (Fig. 12) and the [Ser]/[Ala] values.

The Ripon South and Ripon North opercula are younger than any of the other Holocene sites studied. This places an upper age limit on them of 5000 yr BP as they are younger

than the material from Quidenham Mere, and younger than 6650 BP in comparison with the Enfield Lock material.

The extent of protein decomposition within the Newby Wiske samples is greater than that seen at either level at Quidenham Mere and Enfield Lock, which places a minimum age of about 6650 BP. The protein is less degraded than the Star Carr material, which places a maximum age on these samples of 7640 ± 85 BP.

The Sharow samples are far more degraded than any Holocene samples analysed, but it is likely that these samples have been compromised and no age estimation is attempted.

Conclusions

Out of the 15 samples analysed in this study, only 9 enabled relative age estimations to be determined, using *Bithynia tentaculata* opercula for the sites of Ripon South, Ripon North and Newby Wiske. The 3 opercula samples analysed from Sharow showed that the intra-crystalline fraction of protein had been compromised at some point during the burial history of the samples. This is an extremely unusual occurrence with this material, which has been found to be a particularly robust repository for the original protein, with a normal success rate of recovery of ~97%. Analyses of *Valvata piscinalis* shells were taken from the same layer to investigate this further and the same damage to the intra-crystalline fraction was observed. Therefore no age estimation was possible with the samples from Sharow.

Relative Age

In order of youngest to oldest we would place the sites as follows:

Ripon South: likely to be of a similar age to Ripon North, although perhaps slightly younger, based on the concentration of Asx in the Free fraction which indicates that less protein hydrolysis has occurred within this sample.

Ripon North: This site is similar in age to that of Ripon South and therefore one of the youngest sites analysed in this study. There are indications that the site is slightly older, as the protein is slightly more degraded, as shown by the Free Asx.

Newby Wiske: The samples from Newby Wiske are the oldest uncompromised material from this study. The D/L of Free Asx, Glx, Ser, Ala are all higher than that from the Ripon sites, with a lower [Ser]/[Ala] and generally higher concentrations of Free amino acids, indicating greater protein degradation. The D/L of Hyd Asx, Ser, along with Glx, Ala and Val to a lesser extent, all have increased values compared to the Ripon sites. The [Ser]/[Ala] is also lower.

Sharow: The opercula from Sharow have extremely high levels of racemization in both the Free and Hyd fractions. However, the non-concordance of the Free to Hyd

relationship observed in these samples indicates that they have been compromised and no age estimation is attempted on these samples.

Acknowledgements

Thanks to David Keen, Richard Preece and Petra Dark for supplying the Holocene samples for cross-comparison with the Swale-Ure dataset reported in this study. Funding from NERC, English Heritage and the Wellcome Trust enabled the master dataset of shell and opercula intra-crystalline protein degradation to be developed**.**

References

Abelson, P.H. (1954) Amino acids in fossils. *Science*, **119**, 576.

Abelson, P.H. (1955) Organic constituents of fossils. *Carnegie Institution of Washington Year Book*, **54**, 107–109.

Andrews, J.T., Bowen, D.Q. & Kidson, C. (1979) Amino acid ratios and the correlation of raised beach deposits in south-west England and Wales. *Nature* **281**, 256-258

Bada,. J.L. (1972) The dating of fossil bones using the racemization of isoleucine. *Earth and Planetary Science Letters*, **15**, 223–231.

Bada, J.L. (1982) Racemization of amino acids in nature. *Interdisciplinary Science Reviews*, **7**, 30–46.

Bada, J.L. (1990) Racemization dating. *Science*, **248**, 539–540.

Bada, J.L. (1991) Amino acid cosmogeochemistry. *Philosophical Transactions of the Royal Society, London, Series B*, **333**, 349–358.

Bada, J.L., Shou, M.-Y., Man, E.H. & Schroeder, R.A. (1978) Decomposition of hydroxy amino acids in foraminiferal tests: Kinetics, mechanism and geochronological implications. *Earth and Planetary Science Letters* **41**, 67–76.

Bowen, D.Q., Hughes, S., Sykes, G.A. & Miller, G.H. (1989) Land–sea correlations in the Pleistocene based on isoleucine epimerization in non-marine mollusks. *Nature*, **340**, 49-51.

Chambers, F.M., Mighall, T. & Keen, D.H. (1996) A Holocene pollen and molluscan record from Enfield Lock, Middlesex, U.K. *Proceedings of the Geologists' Association*, **107**, 1–17.

Collins, M.J. (1999) Predicting protein decomposition: the case of aspartic-acid racemization kinetics. *Philosophical Transactions of the Royal Society, London, Series B*, **354**, 51–64.

Goodfriend, G.A. (1991) Patterns of racemization and epimerization of amino acids in land snail shells over the course of the Holocene. *Geochimica et Cosmochimica Acta*, **55**, 293–302.

Goodfriend, G.A. (1992) Rapid racemization of aspartic acid in mollusc shells and potential for dating over recent centuries. *Nature*, **357**, 399–401.

Goodfriend, G.A. & Stanley, D.J. (1996) Reworking and discontinuities in Holocene sedimentation in the Nile Delta – documentation from amino-acid racemization and stable isotopes in mollusk shells. *Marine Geology*, **129**, 271–283.

Harada, N., Handa, N., Ito, M., Oba, T. & Matsumoto, E. (1996) Chronology of marine sediments by the racemization reaction of aspartic acid in planktonic foraminifera. *Organic Geochemistry*, **24**, 921–930.

Hare, P.E. & Abelson, P.H. (1967) Racemization of amino acids in fossil shells. *Carnegie Institution of Washington Year Book*, **66**, 526–528.

Hare, P.E. & Mitterer, R.M. (1969) Laboratory simulation of amino-acid diagenesis in fossils. *Carnegie Institution of Washington Year Book*, **67**, 205–208.

Hare, P.E., von Endt, D.W. & Kokis, J.E. (1997) Protein and amino acid diagenesis dating. In: *Chronometric Dating in Archaeology. Advances in Archaeological and Museum Science, 2* (eds R.E. Taylor & M.J. Aitken), pp. 261–296. Plenum Press, New York.

Hill, R.L. (1965) Hydrolysis of proteins. *Advances in Protein Chemistry*, **20**, 37–107.

Howard, A.J., Keen, D.H., Mighall, T.M., Field, M.H., Coope, G.R., Griffiths, H.I. & Macklin, M.G. (2000a) Early Holocene environments of the River Ure near Ripon, North Yorkshire, UK. *Proceedings of the Yorkshire Geological Society*, **53**, 31–42.

Johnson, B.J. & Miller, G.H. (1997) Archaeological applications of amino acid racemization. *Archaeometry*, **39**, 265–287.

Kaufman, D.S. (2000) Amino Acid Racemization in Ostracods. In: *Perspectives in Amino Acid and Protein Geochemistry* (eds G.A. Goodfriend, M.J. Collins, M.L. Fogel, S.A. Macko, & J.F. Wehmiller), pp. 145–160. Oxford University Press.

Kaufman, D.S. & Manley, W.F. (1998) A new procedure for determining DL amino acid ratios in fossils using Reverse Phase Liquid ChromatographyA new procedure for determining DL amino acid ratios in fossils using Reverse Phase Liquid Chromatography. *Quaternary Science Reviews*, **17**, 987–1000.

Lajoie, K.R., Peterson, E. & Gerow, B.A. (1980) Amino acid bone dating: a feasibility study, South San Francisco Bay region, California. In: *Biogeochemistry of amino acids* (eds P.E. Hare, T.C. Hoering, & K.J. King), pp. 477–489. John Wiley, New York.

Lauritzen, S.E., Haugen, J.E., Lovlie, R. & Giljenielsen, H. (1994) Geochronological Potential of Isoleucine Epimerization in Calcite Speleothems. *Quaternary Research*, **41**, 52–58.

Marshall, E. (1990) Racemization dating: great expectations. *Science*, **247**, 799.

Mellars, P. & Dark, P. (1998) *Star Carr in Context: New Archaeological and Palaeoecological Investigations at the Early Mesolithic Site of Star Carr, North Yorkshire*. McDonald Institute for Archaeological Research, Cambridge

Miller, G.H., Hollin, J.T. & Andrews, J.T. (1979) Aminostratigraphy of UK Pleistocene deposits. *Nature* **281** (5732), 539-543

Miller, G.H., Beaumont, P.B., Jull, A.J.T. & Johnson, B. (1992) Pleistocene geochronology and palaeothermometry from protein diagenesis in ostrich eggshells: implications for the evolution of modern humans. *Philosophical Transactions of the Royal Society*, *London*, *Series B*. **337**, 149-157

Miller, G.H., Hart, C.P., Roark, E.B. & Johnson, B.J. (2000) Isoleucine epimerization in eggshells of the flightless Australian birds *Genyornis* and *Dromaius*. In: *Perspectives in Amino Acid and Protein Geochemistry* (eds G.A. Goodfriend, M.J. Collins, M.L. Fogel, S.A. Macko, & J.F. Wehmiller), pp. 161–181. Oxford University Press.

Miller, G.H., Magee, J.W. & Jull, A.J.T. (1997) Low-latitude glacial cooling in the Southern Hemisphere from amino acid racemization in emu eggshells. *Nature*, **385**, 241–244.

Murray-Wallace, C.V. (1993) A review of the application of the amino acid racemisation reaction to archaeological dating. *The Artefact*, **16**, 19–26.

Murray-Wallace, C.V. & Kimber, R.W.L. (1987) Evaluation of the amino acid racemization reaction in studies of Quaternary marine sediments in South Australia. *Australian Journal of Earth Sciences*, **34**, 279–292.

Parfitt, S.A., Barendregt, R.W., Breda, M., Candy, I., Collins, M.J., Coope, G.R., Durbidge, P., Field, M.H., Lee, J.R., Lister, A.M., Mutch, R., Penkman, K.E.H., Preece, R.C., Rose, J., Stringer, C.B., Symmons, R., Whittaker, J.E., Wymer, J.J & Stuart, A.J. (2005) The earliest humans in Northern Europe: artefacts from the Cromer Forest-bed Formation at Pakefield, Suffolk, UK. *Nature*, **438**, 1008–1012

Penkman, K.E.H. (2005) *Amino acid geochronology: a closed system approach to test and refine the UK model*. Unpublished PhD. Thesis, University of Newcastle-upon-Tyne.

Penkman, K.E.H., Preece, R.C., Keen, D.H., Maddy, D., Schreve, D.C. & Collins, M. (2007). Testing the aminostratigraphy of fluvial archives: the evidence from intra-crystalline proteins within freshwater shells. *Quaternary Science Reviews*, **26**, 2958–2969.

Penkman, K.E.H., Kaufman, D.S., Maddy, D. & Collins, M.J. (2008a) Closed-system behaviour of the intra-crystalline fraction of amino acids in mollusc shells. *Quaternary Geochronology,* **3**, 2-25.

Penkman, K., Preece, R.C., Keen, D.H. & Collins, M. (2008b) British aggregates: An improved chronology using amino acid racemization and degradation of intra-crystalline amino acids (IcPD). *English Heritage Research Department Report Series* 6/2008

Penkman, K.E.H., Preece, R.C., Keen, D.H. & Collins, M.J. (in press). Amino acid geochronology of the type Cromerian of West Runton, Norfolk, UK. *Quaternary International*

Preece, R.C. & Penkman, K. (2005) New faunal analyses and amino acid dating of the Lower Palaeolithic site at East Farm, Barnham, Suffolk. *Proceedings of the Geologists' Association*, **116**, 363–378.

Rutter, N.W. & Blackwell, B. (1995) Amino acid racemization dating. In: *Dating methods for Quaternary deposits* (eds N.W. Rutter & N.R. Catto), pp. 125–164. Geological Association of Canada, St. John's, Newfoundland.

Schroeder, R.A. & Bada, J.L. (1976) A review of the geochemical applications of the amino acid racemization reaction. *Earth-Science Reviews*, **12**, 347–391.

Smith, G.G. & Evans, R.C. (1980) The effect of structure and conditions on the rate of racemization of free and bound amino acids. In: *Biogeochemistry of amino acids* (eds P.E. Hare, T.C. Hoering & J. King) pp. 257–282. John Wiley, New York.

Sykes, G.A., Collins, M.J. & Walton, D.I. (1995) The significance of a geochemically isolated intracrystalline organic fraction within biominerals. *Organic Geochemistry*, **11/12**, 389–410.

Walton, D.I. (1998) Degradation of intracrystalline proteins and amino acids in fossil brachiopods. *Organic Geochemistry*, **28**, 389–410.

Supplement 1

Glossary

18MΩ water: The water has a resistivity of 18MΩ/cm, indicating a lack of ions.

HPLC grade water: In addition to low ion content, HPLC grade water has a low organic content (typically < 2 ppb).

Amino acids: the building blocks of proteins and consist of an alpha carbon atom (C_α) which has four different groups bonded to it: an amino group ($-NH_2$), a carboxyl group (-COOH), a hydrogen atom (-H), and a side chain, (often called an R group). About 20 amino acids normally occur in nature and some of these can undergo further modification (e.g. the hydroxylation of proline to hydroxyproline). The amino acids are commonly known by three letter codes (see Supplement 3: Abbreviations). They exist free in the cell, but are more commonly linked together by peptide bonds to form proteins, peptides, and sub-components of some other macromolecules (e.g. bacterial peptidoglycan).

Amino acid isomers: amino acids occur as two stereoisomers that are chemically identical, but optically different. These isomers are designated as either D (dextro-rotary) or L (laevo-rotary) depending upon whether they rotate plane polarised light to the right or left respectively (Fig 6). In living organisms the amino acids in protein are almost exclusively L and the D/L ratio approaches zero. Two amino acids, isoleucine and threonine, have two chiral carbon atoms and therefore have four stereoisomers each. As well as racemization, these two amino acids can undergo a process known as epimerization. The detection of the L-alloisoleucine epimer (derived from L-isoleucine) is possible by conventional ion-exchange chromatography, and was thus the most commonly used reaction pathway in geochronology.

Asx: Measurements of aspartic acid following hydrolysis also include asparagine, which decomposes to Asx. This combined signal of aspartic acid plus asparagine (Asp +Asn) is referred to as Asx (Hill, 1965).

D-amino acid: dextrorotary amino acid, formed following synthesis of the protein as it degrades over time (remember as ‘dead amino acid’).

IcPD: Intra-crystalline Protein Degradation. This is the measure of the overall extent of protein breakdown in the closed system of the intra-crystalline fraction of a shell. The IcPD value is a summary value obtained from multiple amino acid D/L values from a single sample all normalised to a common model of protein degradation and racemization.

Enantiomers / optical isomers: mirror image forms of the same compound that cannot be superimposed on one another.

Epimerisation: the inversion of the chiral α-carbon atom.

Free amino acid fraction: The fraction of amino acids directly amenable to racemization analysis. Only amino acids which have already been naturally hydrolysed (over time) are measured. These are the most highly racemized amino acids.

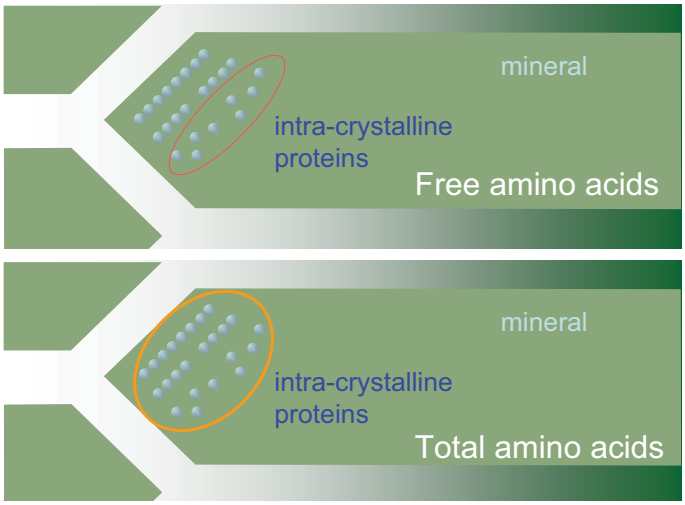

Hydrolysis: A chemical reaction involving water leading to the breaking apart of a compound (in this case the breaking of peptide bonds to release amino acids).

L-amino acid: laevorotary amino acid, the constituent form of proteins (remember as 'living amino acid').

Peptide bond: an amide linkage between the carboxyl group of one amino acid and the amino group of another.

Racemization: the inversion of all chiral carbon atoms, leading to the decrease in specific optical rotation. When the optical rotation is reduced to zero, the mixture is said to be racemized.

Stereoisomers: molecules of the same compound that have their atoms arranged differently in space.

Total amino acid fraction: The extent of racemization of all amino acids in a sample, determined following aggressive high temperature hydrolysis with strong mineral acid, which has the effect of breaking apart all peptide bonds so that the total extent of racemization in all amino acids both free and peptide bound are measured. Also referred to as “Hydrolysed” or “Hyd”.

Zwitterion: A dipolar ion containing ionic groups of opposite charge. At neutral pH the ionic form of amino acids which predominates is the zwitterions

Supplement 2

Past Use of Amino Acid Racemization Dating.

The presence of proteins in archaeological remains has been known for some time; nearly fifty years ago Abelson (1954) separated amino acids from subfossil shell. He suggested the possibility of using the kinetics of the degradation of amino acids as the basis for a dating method (Abelson, 1955). In the mid-1960s Hare and Abelson measured the extent of degradation by racemization of amino acids extracted from modern and sub-fossil *Mercenaria mercenaria* (edible clam) shells. They found that the total amount of amino acids present decreased with the age of the shell and that the amino acids in recent shell were all in the L-configuration, but over time the amount of D-configuration amino acid increased as a result of racemization (Hare & Abelson, 1967). This chemical reaction is the basis of Amino Acid Racemization dating (AAR). However, even after 35 years this method is still subject to vigorous debate, with its application to date bone being particularly controversial (Bada, 1990; Marshall, 1990). Detailed reviews of AAR include those by Schroeder and Bada (1976), Bada (1991), Murray-Wallace (1993), Rutter and Blackwell (1995), Johnson and Miller (1997) and Hare *et al*. (1997).

The rate of racemization is influenced by a number of factors, including amino acid structure, the sequence of amino acids in peptides, pH, buffering effects, metallic cations, the presence of water and temperature. To establish a dating method the kinetics and mechanisms of the racemization reaction of free- and peptide-bound amino acids need to be established. To this end, various workers in the late 1960s and the 1970s studied free amino acids in solution and carried out laboratory simulations of post-mortem changes in the amino acids in bone (Bada, 1972) and shell (Hare & Abelson, 1967; Hare & Mitterer, 1969). Attempts have also been made to relate the kinetics of free amino acids to those in short polypeptides and the proteins in various archaeological samples (Bada, 1982; Smith & Evans, 1980). The suitability of this technique as a geochronological and geothermometry tool has led to its use in many environmental studies, on a range of substrates from terrestrial gastropods (e.g. Goodfriend, 1991; 1992), bivalves (e.g. Goodfriend & Stanley, 1996), foraminifera (Harada *et al*., 1996), ostrich egg shells (Miller *et al*., 1992, 1997) and speleothems (Lauritzen *et al*., 1994). Early methods of

chemical separation, using Ion-Exchange Liquid Chromatography, were able to separate the enantiomers of one amino acid found in proteins, L-isoleucine (L-Ile, I), from its most stable diastereoisomer alloisoleucine (D-aile, A). By analysing the total protein content within mollusc shells from interglacial sites, an amino acid geochronology begun to be developed for the UK using the increase in A/I observed (Miller *et al*., 1979; Andrews *et al*., 1979), with correlations made with the marine oxygen isotope warm stages (Bowen *et al*., 1989).

Supplement 3

Abbreviations used in amino acid reports

Abbrev	1-letter code	number of chiral centres	
Ala	A	1	Alanine
Arg	R	1	Arginine
ACN			acetonitrile
AA			Amino acid(n)
Asn	N	1	Asparagine
Asp	D	1	Aspartic acid
Asx			Asparagine + Aspartic acid + succinimide
Asu			Succinimide
Cys	C	1	Cysteine
DCM			Dichlormethane
GABA			γ-Aminobutyric acid
Gln	Q	1	Glutamine
Glu	E	1	Glutamic acid
Gly	G	0	Glycine
His	H	1	Histidine
HPLC			High-Performance Liquid Chromatography
Hyp			Hydroxyproline
IBD(L)C			N-Isobutyryl-D(L)-Cysteine
Ile	I	2	Isoleucine
Leu	L	1	Leucine
Lys	K	1	Lysine
MeOH			Methanol
Met	M	1	Methionine
Nle			Norleucine
OPA			ortho-Phthaldialdehyde
Orn			Ornithine
Phe	F	1	Phenylalanine
Pro	P	1	Proline
Ser	S	1	Serine
Thr	T	2	Threonine
Trp	W	1	Tryptophan
Tyr	Y	1	Tyrosine
Val	V	1	Valine

Supplement 4

Data sheets from the Swale-Ure

NEaar	File	Genus	Species	materials	location	Type	Asx conc pmol/mg	Glx conc pmol/mg	Ser conc pmol/mg	Gly conc pmol/mg	Ala conc pmol/mg	Val conc pmol/mg
3105bF	G205-0812	*Bithynia*	*tentaculata*	operculum	Ripon Racecourse, 2/10/3 OSL	F	22	6	127	81	35	10
3105bF	G205-0828	*Bithynia*	*tentaculata*	operculum	Ripon Racecourse, 2/10/3 OSL	F	24	7	126	83	32	14
3105bH*	G207-1613	*Bithynia*	*tentaculata*	operculum	Ripon Racecourse, 2/10/3 OSL	H*	2263	1570	1513	4800	2026	1118
3105bH*	G207-1630	*Bithynia*	*tentaculata*	operculum	Ripon Racecourse, 2/10/3 OSL	H*	2083	1346	1534	4554	1935	1160
3106bF	G205-3072	*Bithynia*	*tentaculata*	operculum	Ripon Racecourse, 2/10/3 OSL	F	15	0	61	97	18	0
3106bF	G205-3083	*Bithynia*	*tentaculata*	operculum	Ripon Racecourse, 2/10/3 OSL	F	15	0	68	91	19	0
3106bH*	G208-0928	*Bithynia*	*tentaculata*	operculum	Ripon Racecourse, 2/10/3 OSL	H*	2121	1336	1300	3448	1392	1022
3106bH*	G209-0908	*Bithynia*	*tentaculata*	operculum	Ripon Racecourse, 2/10/3 OSL	H*	1987	1224	1313	3337	1414	1064
3107bF	G205-43A3	*Bithynia*	*tentaculata*	operculum	Ripon Racecourse, 2/10/3 OSL	F	19	0	57	131	25	0
3107bF	G205-43AM	*Bithynia*	*tentaculata*	operculum	Ripon Racecourse, 2/10/3 OSL	F	18	0	56	130	119	0
3107bH*	G209-1715	*Bithynia*	*tentaculata*	operculum	Ripon Racecourse, 2/10/3 OSL	H*	1111	718	808	2814	864	485
3107bH*	G209-1722	*Bithynia*	*tentaculata*	operculum	Ripon Racecourse, 2/10/3 OSL	H*	1080	654	805	2665	896	485
3108bF	G205-44A4	*Bithynia*	*tentaculata*	operculum	Hansons/Ripon, 1.1	F	24	6	147	82	34	10
3108bF	G205-44AN	*Bithynia*	*tentaculata*	operculum	Hansons/Ripon, 1.1	F	23	6	147	80	40	10
3108bH*	G207-1731	*Bithynia*	*tentaculata*	operculum	Hansons/Ripon, 1.1	H*	3254	1856	1763	3952	1902	1238
3108bH*	G207-1738	*Bithynia*	*tentaculata*	operculum	Hansons/Ripon, 1.1	H*	3453	1964	1845	4046	1983	1305
3109bF	G206-0103	*Bithynia*	*tentaculata*	operculum	Hansons/Ripon, 1.1	F	25	8	166	84	37	12
3109bF	G206-0110	*Bithynia*	*tentaculata*	operculum	Hansons/Ripon, 1.1	F	25	7	164	78	35	8
3109bH*	G208-1029	*Bithynia*	*tentaculata*	operculum	Hansons/Ripon, 1.1	H*	3139	1753	1792	4801	1797	979
3109bH*	G209-1009	*Bithynia*	*tentaculata*	operculum	Hansons/Ripon, 1.1	H*	3151	1740	1779	4607	1792	986
3110bF	G207-1006	*Bithynia*	*tentaculata*	operculum	Hansons/Ripon, 1.1	F	27	7	167	83	36	11
3110bF	G207-1022	*Bithynia*	*tentaculata*	operculum	Hansons/Ripon, 1.1	F	28	7	168	84	37	13
3110bH*	G209-1816	*Bithynia*	*tentaculata*	operculum	Hansons/Ripon, 1.1	H*	1728	1035	884	1984	994	652
3110bH*	G209-1823	*Bithynia*	*tentaculata*	operculum	Hansons/Ripon, 1.1	H*	1757	1056	899	2072	1006	667

NEaar	File	Genus	Species	materials	location	Type	Asx conc pmol/mg	Glx conc pmol/mg	Ser conc pmol/mg	Gly conc pmol/mg	Ala conc pmol/mg	Val conc pmol/mg
3123bF	G205-45A5	*Bithynia*	*tentaculata*	operculum	Newby Wiske, 1 220-230	F	224	66	493	469	326	112
3123bF	G205-45AO	*Bithynia*	*tentaculata*	operculum	Newby Wiske, 1 220-230	F	222	63	487	448	326	109
3123bH*	G207-1832	*Bithynia*	*tentaculata*	operculum	Newby Wiske, 1 220-230	H*	2824	1794	1438	4454	2103	1144
3123bH*	G207-1839	*Bithynia*	*tentaculata*	operculum	Newby Wiske, 1 220-230	H*	2889	1817	1437	4360	2131	1172
3124bF	G206-0204	*Bithynia*	*tentaculata*	operculum	Newby Wiske, 1 220-230	F	238	64	555	430	313	90
3124bF	G206-0211	*Bithynia*	*tentaculata*	operculum	Newby Wiske, 1 220-230	F	237	63	566	435	312	91
3124bH*	G209-1202	*Bithynia*	*tentaculata*	operculum	Newby Wiske, 1 220-230	H*	2617	1597	1203	3691	1602	989
3124bH*	G209-1210	*Bithynia*	*tentaculata*	operculum	Newby Wiske, 1 220-230	H*	2587	1568	1201	3699	1607	997
3125bF	G207-1107	*Bithynia*	*tentaculata*	operculum	Newby Wiske, 1 220-230	F	158	49	376	325	234	71
3125bF	G207-1123	*Bithynia*	*tentaculata*	operculum	Newby Wiske, 1 220-230	F	158	49	373	297	232	71
3125bH*	G209-1917	*Bithynia*	*tentaculata*	operculum	Newby Wiske, 1 220-230	H*	3065	1847	1511	4145	1949	1146
3125bH*	G209-1924	*Bithynia*	*tentaculata*	operculum	Newby Wiske, 1 220-230	H*	3046	1814	1509	4123	1866	1156
3126bF	G205-46A6	*Bithynia*	*tentaculata*	operculum	Sharow, 560-570	F	773	109	43	1435	1114	388
3126bF	G205-46AP	*Bithynia*	*tentaculata*	operculum	Sharow, 560-570	F	767	106	43	1291	1112	390
3126bH*	G207-1933	*Bithynia*	*tentaculata*	operculum	Sharow, 560-570	H*	2150	1767	363	3693	2034	1068
3126bH*	G207-1940	*Bithynia*	*tentaculata*	operculum	Sharow, 560-570	H*	2155	1768	362	3592	2042	1072
3127bF	G206-0305	*Bithynia*	*tentaculata*	operculum	Sharow, 560-570	F	633	80	31	1111	826	280
3127bF	G206-0312	*Bithynia*	*tentaculata*	operculum	Sharow, 560-570	F	632	78	30	1080	823	282
3127bH*	G209-1303	*Bithynia*	*tentaculata*	operculum	Sharow, 560-570	H*	1505	1146	281	2302	1248	751
3127bH*	G209-1311	*Bithynia*	*tentaculata*	operculum	Sharow, 560-570	H*	1495	1139	280	2258	1236	753
3128bF	G207-1208	*Bithynia*	*tentaculata*	operculum	Sharow, 560-570	F	771	92	37	962	909	322
3128bF	G207-1224	*Bithynia*	*tentaculata*	operculum	Sharow, 560-570	F	774	90	38	858	914	325
3128bH*	G209-2018	*Bithynia*	*tentaculata*	operculum	Sharow, 560-570	H*	1869	1424	348	3191	1694	801
3128bH*	G209-2025	*Bithynia*	*tentaculata*	operculum	Sharow, 560-570	H*	1876	1430	348	3100	1663	803

NEaar	File	Genus	Species	materials	location	Type	Asx conc pmol/mg	Glx conc pmol/mg	Ser conc pmol/mg	Gly conc pmol/mg	Ala conc pmol/mg	Val conc pmol/mg
3303bF	G215-0409	*Valvata*	*piscinalis*	shell	Sharow, 560-570	F	98	28	4	465	183	56
3303bF	G215-0419	*Valvata*	*piscinalis*	shell	Sharow, 560-570	F	100	27	4	211	177	58
3303bH*	G215-0712	*Valvata*	*piscinalis*	shell	Sharow, 560-570	H*	231	242	47	764	281	108
3303bH*	G215-0722	*Valvata*	*piscinalis*	shell	Sharow, 560-570	H*	236	240	29	416	271	111
3304bF	G215-0510	*Valvata*	*piscinalis*	shell	Sharow, 560-570	F	121	30	10	557	210	54
3304bF	G215-0520	*Valvata*	*piscinalis*	shell	Sharow, 560-570	F	122	30	11	546	210	55
3304bH*	G215-0813	*Valvata*	*piscinalis*	shell	Sharow, 560-570	H*	270	280	75	744	329	129
3304bH*	G215-0823	*Valvata*	*piscinalis*	shell	Sharow, 560-570	H*	280	280	49	446	322	132
3305bF	G215-0611	*Valvata*	*piscinalis*	shell	Sharow, 560-570	F	101	27	6	319	163	55
3305bF	G215-0621	*Valvata*	*piscinalis*	shell	Sharow, 560-570	F	103	27	5	170	160	57
3305bH*	G215-0914	*Valvata*	*piscinalis*	shell	Sharow, 560-570	H*	205	202	26	568	239	95
3305bH*	G215-0925	*Valvata*	*piscinalis*	shell	Sharow, 560-570	H*	216	203	19	333	236	102

NEaar	Genus	materials	location	Phe conc pmol/mg	Leu conc pmol/mg	Ile conc pmol/mg	Asx D/L	Glx D/L	Ser D/L	Ala D/L	Val D/L	[Ser]/[Ala]
3105bF	*Bithynia*	operculum	Ripon Racecourse, 2/10/3 OSL	5	9	8	0.169	0.000	0.274	0.124	0.439	3.600
3105bF	*Bithynia*	operculum	Ripon Racecourse, 2/10/3 OSL	9	11	8	0.198	0.000	0.275	0.094	0.526	3.942
3105bH*	*Bithynia*	operculum	Ripon Racecourse, 2/10/3 OSL	572	1285	467	0.176	0.043	0.131	0.066	0.028	0.747
3105bH*	*Bithynia*	operculum	Ripon Racecourse, 2/10/3 OSL	530	1386	469	0.179	0.044	0.130	0.032	0.028	0.793
3106bF	*Bithynia*	operculum	Ripon Racecourse, 2/10/3 OSL	13	0	28	0.000	ND	0.000	0.000	ND	3.441
3106bF	*Bithynia*	operculum	Ripon Racecourse, 2/10/3 OSL	0	0	25	0.000	ND	0.137	0.000	ND	3.619
3106bH*	*Bithynia*	operculum	Ripon Racecourse, 2/10/3 OSL	470	1147	481	0.128	0.045	0.102	0.033	0.023	0.934
3106bH*	*Bithynia*	operculum	Ripon Racecourse, 2/10/3 OSL	433	1150	499	0.132	0.045	0.103	0.029	0.026	0.928
3107bF	*Bithynia*	operculum	Ripon Racecourse, 2/10/3 OSL	31	0	62	0.000	ND	0.000	0.000	ND!	2.262
3107bF	*Bithynia*	operculum	Ripon Racecourse, 2/10/3 OSL	0	0	64	0.000	ND	0.000	0.629	ND	0.467
3107bH*	*Bithynia*	operculum	Ripon Racecourse, 2/10/3 OSL	240	547	199	0.165	0.049	0.108	0.024	0.000	0.935
3107bH*	*Bithynia*	operculum	Ripon Racecourse, 2/10/3 OSL	182	592	178	0.162	0.047	0.106	0.039	0.000	0.899
3108bF	*Bithynia*	operculum	Hansons/Ripon, 1.1	6	9	5	0.149	0.000	0.287	0.069	0.303	4.308
3108bF	*Bithynia*	operculum	Hansons/Ripon, 1.1	5	8	5	0.137	0.000	0.288	0.141	0.362	3.674
3108bH*	*Bithynia*	operculum	Hansons/Ripon, 1.1	520	1507	521	0.183	0.048	0.168	0.042	0.021	0.927
3108bH*	*Bithynia*	operculum	Hansons/Ripon, 1.1	535	1591	536	0.183	0.048	0.169	0.032	0.020	0.930
3109bF	*Bithynia*	operculum	Hansons/Ripon, 1.1	7	19	6	0.150	0.000	0.267	0.079	0.349	4.434
3109bF	*Bithynia*	operculum	Hansons/Ripon, 1.1	7	8	5	0.135	0.000	0.263	0.060	0.000	4.660
3109bH*	*Bithynia*	operculum	Hansons/Ripon, 1.1	437	1096	351	0.196	0.050	0.167	0.033	0.022	0.997
3109bH*	*Bithynia*	operculum	Hansons/Ripon, 1.1	437	1092	354	0.197	0.049	0.167	0.032	0.020	0.993
3110bF	*Bithynia*	operculum	Hansons/Ripon, 1.1	8	9	12	0.137	0.000	0.275	0.064	0.306	4.606
3110bF	*Bithynia*	operculum	Hansons/Ripon, 1.1	7	9	8	0.148	0.000	0.273	0.079	0.446	4.537
3110bH*	*Bithynia*	operculum	Hansons/Ripon, 1.1	284	791	284	0.179	0.051	0.165	0.039	0.018	0.889
3110bH*	*Bithynia*	operculum	Hansons/Ripon, 1.1	290	810	285	0.181	0.051	0.165	0.032	0.017	0.894

NEaar	Genus	materials	location	Phe conc pmol/mg	Leu conc pmol/mg	Ile conc pmol/mg	Asx D/L	Glx D/L	Ser D/L	Ala D/L	Val D/L	[Ser]/[Ala]
3123bF	*Bithynia*	operculum	Newby Wiske, 1 220-230	45	87	27	0.339	0.097	0.520	0.089	0.119	1.513
3123bF	*Bithynia*	operculum	Newby Wiske, 1 220-230	36	91	25	0.341	0.096	0.520	0.096	0.111	1.490
3123bH*	*Bithynia*	operculum	Newby Wiske, 1 220-230	547	1421	479	0.349	0.065	0.319	0.065	0.040	0.684
3123bH*	*Bithynia*	operculum	Newby Wiske, 1 220-230	539	1457	494	0.352	0.065	0.325	0.065	0.041	0.674
3124bF	*Bithynia*	operculum	Newby Wiske, 1 220-230	41	93	29	0.363	0.091	0.566	0.103	0.162	1.771
3124bF	*Bithynia*	operculum	Newby Wiske, 1 220-230	44	100	33	0.366	0.103	0.571	0.103	0.172	1.813
3124bH*	*Bithynia*	operculum	Newby Wiske, 1 220-230	418	1154	395	0.334	0.066	0.308	0.057	0.033	0.751
3124bH*	*Bithynia*	operculum	Newby Wiske, 1 220-230	419	1160	398	0.334	0.065	0.308	0.056	0.032	0.748
3125bF	*Bithynia*	operculum	Newby Wiske, 1 220-230	29	63	18	0.322	0.086	0.547	0.098	0.151	1.607
3125bF	*Bithynia*	operculum	Newby Wiske, 1 220-230	30	67	17	0.327	0.103	0.539	0.102	0.150	1.608
3125bH*	*Bithynia*	operculum	Newby Wiske, 1 220-230	532	1430	481	0.325	0.062	0.302	0.079	0.035	0.775
3125bH*	*Bithynia*	operculum	Newby Wiske, 1 220-230	503	1418	482	0.327	0.062	0.304	0.059	0.034	0.809
3126bF	*Bithynia*	operculum	Sharow, 560-570	143	347	139	0.922	0.591	0.483	0.930	0.779	0.039
3126bF	*Bithynia*	operculum	Sharow, 560-570	141	331	141	0.917	0.586	0.517	0.928	0.776	0.038
3126bH*	*Bithynia*	operculum	Sharow, 560-570	447	1162	440	0.473	0.365	0.211	0.458	0.304	0.179
3126bH*	*Bithynia*	operculum	Sharow, 560-570	446	1201	455	0.471	0.364	0.210	0.464	0.305	0.177
3127bF	*Bithynia*	operculum	Sharow, 560-570	88	261	109	0.921	0.538	0.494	0.932	0.766	0.037
3127bF	*Bithynia*	operculum	Sharow, 560-570	94	258	107	0.924	0.545	0.504	0.930	0.758	0.036
3127bH*	*Bithynia*	operculum	Sharow, 560-570	316	843	353	0.493	0.350	0.191	0.460	0.251	0.225
3127bH*	*Bithynia*	operculum	Sharow, 560-570	312	837	349	0.492	0.351	0.189	0.459	0.254	0.226
3128bF	*Bithynia*	operculum	Sharow, 560-570	92	321	108	0.925	0.554	0.546	0.922	0.761	0.041
3128bF	*Bithynia*	operculum	Sharow, 560-570	89	301	108	0.923	0.548	0.593	0.919	0.755	0.042
3128bH*	*Bithynia*	operculum	Sharow, 560-570	345	887	305	0.512	0.374	0.206	0.503	0.334	0.206
3128bH*	*Bithynia*	operculum	Sharow, 560-570	337	891	302	0.512	0.375	0.211	0.500	0.332	0.209

NEaar	Genus	materials	location	Phe conc pmol/mg	Leu conc pmol/mg	Ile conc pmol/mg	Asx D/L	Glx D/L	Ser D/L	Ala D/L	Val D/L	[Ser]/[Ala]
3303bF	*Valvata*	shell	Sharow, 560-570	56	147	40	0.828	0.588	0.000	0.856	0.689	0.024
3303bF	*Valvata*	shell	Sharow, 560-570	54	141	37	0.829	0.596	0.000	0.849	0.671	0.025
3303bH*	*Valvata*	shell	Sharow, 560-570	103	270	70	0.639	0.356	0.070	0.602	0.379	0.167
3303bH*	*Valvata*	shell	Sharow, 560-570	97	261	70	0.639	0.356	0.000	0.585	0.357	0.107
3304bF	*Valvata*	shell	Sharow, 560-570	57	149	45	0.796	0.547	0.000	0.830	0.637	0.049
3304bF	*Valvata*	shell	Sharow, 560-570	56	147	42	0.805	0.575	0.000	0.822	0.610	0.050
3304bH*	*Valvata*	shell	Sharow, 560-570	120	285	91	0.430	0.261	0.048	0.370	0.186	0.228
3304bH*	*Valvata*	shell	Sharow, 560-570	111	276	91	0.432	0.260	0.000	0.366	0.177	0.151
3305bF	*Valvata*	shell	Sharow, 560-570	52	134	36	0.841	0.645	0.543	0.835	0.618	0.037
3305bF	*Valvata*	shell	Sharow, 560-570	52	132	36	0.832	0.615	0.514	0.834	0.603	0.033
3305bH*	*Valvata*	shell	Sharow, 560-570	91	226	65	0.612	0.377	0.156	0.591	0.383	0.111
3305bH*	*Valvata*	shell	Sharow, 560-570	92	223	71	0.608	0.374	0.156	0.569	0.374	0.079